frontiers | Frontiers in Earth Science

TYPE Original Research
PUBLISHED 23 December 2022
DOI 10.3389/feart.2022.898843

OPEN ACCESS

EDITED BY
Hema Achyuthan,
Anna University, India

REVIEWED BY
Andrew Green,
University of KwaZulu-Natal, South Africa
Aasif Mohmad Lone,
Indian Institute of Science Education and Research, India

*CORRESPONDENCE
Achim Wehrmann,
achim.wehrmann@senckenberg.de

SPECIALTY SECTION
This article was submitted to Quaternary Science, Geomorphology and Paleoenvironment, a section of the journal Frontiers in Earth Science

RECEIVED 17 March 2022
ACCEPTED 21 November 2022
PUBLISHED 23 December 2022

CITATION
Schüller I, Belz L, Wilkes H and Wehrmann A (2022), Sedimentary evolution of lagoons along the Namibian coast reveals fluctuation in Holocene biogeographic faunal provinces, upwelling intensity and sea level.
Front. Earth Sci. 10:898843.
doi: 10.3389/feart.2022.898843

Sedimentary evolution of lagoons along the Namibian coast reveals fluctuation in Holocene biogeographic faunal provinces, upwelling intensity and sea level

Irka Schüller[1], Lukas Belz[2,3], Heinz Wilkes[2,3] and Achim Wehrmann[1]*

[1]Marine Research Department, Senckenberg am Meer, Wilhelmshaven, Germany, [2]Institute for Chemistry and Biology of the Marine Environment, Carl von Ossietzky University of Oldenburg, Oldenburg, Germany, [3]Helmholtz Centre Potsdam, GFZ German Research Centre for Geosciences, Potsdam, Germany

Within the wave-dominated and high-energy depositional environment of the hyper-arid Namibian coast, lagoons and related saltpans represent one of the few regional settings in which sediments originating from both marine and terrestrial sources can accumulate under sheltered conditions. This allows for an approximately continuous depositional record of mid to late Holocene coastal evolution. For this paleoenvironmental reconstruction, 26 sediment cores from six coastal (paleo-) lagoons were taken and investigated along a 430 km-long latitudinal gradient. Based on 56 age determinations of sediments and shell material, the initial formation of the studied lagoons can be dated back to 6.0–5.3 cal kyr BP. The sediment cores present different types of lithoclastic sediments which can be assigned to five sedimentary facies ranging from sand spit sediments rich in shell material to eolian dune sands and evaporites. From these cores, 221 samples of macrobenthic faunal material have been collected and determined to possess 46 shallow marine species. Biogeographic analyses have resulted in the identification of 10 (sub-)tropical warm water species that are not part of the regional benthic fauna in the present upwelling system. Age determinations of the shell material revealed four phases of biogeographic range expansion/shift into the study area, at 5.3 cal kyr BP, 2.8 cal kyr BP, 1.2–0.9 cal kyr BP, and 0.36–0.12 cal kyr BP from both the northern tropical Angola Current as well as from the southern subtropical Agulhas Current. The combination of datasets from this study with published datasets of regional sea-level fluctuations and upwelling intensities presents an apparent correlation between both processes and presumably an additional linkage to the ENSO and Benguela Niño variability.

KEYWORDS

coastal pans, macrobenthos, palaeoenvironment, longshore currents, Benguela, Quaternary, South Atlantic Ocean

1 Introduction

The Namibian coast is characterized by extreme environmental conditions which are caused and controlled by the complex interaction of oceanographic and atmospheric processes. Due to a semi- to hyper-arid climate, the coastal hinterland consists of a distinctive sand erg in the Namib and a monotonous rock desert at the Skeleton Coast. The rarity of continuous geoarchives in these areas limits the reconstruction of the post-glacial evolution of the coastal zone and the estimation of its resilience and sensitivity to future changes in predicted climatic and environmental conditions. However, coastal lagoons and related pans, as well as wetlands (vleis), provide valuable records of Holocene paleoenvironmental information, for example, sea-level changes, fluctuations in upwelling strength, and other climatic signals (Miller et al., 1993; Baxter and Meadows, 1999; Compton, 2001; Compton, 2006; Compton, 2007).

Along the Atlantic coast of South Africa and Namibia, few detailed studies about the fossil to recent coastal faunal have been performed (Compton, 2007). The occurrence of (sub-) tropical species in the recently cool-temperate upwelling areas is of particular interest for regional research as it is assumingly connected with faunal range expansions during phases of weak upwelling and the advection of warm and low-nutrient water masses from the Angola Current and Agulhas Current. Tankard (1975) detected a southward migration of selected West African bivalves during the previous interglacial (125 kaBP) through the Benguela upwelling barrier into warm, sheltered embayments along the Cape coast. Kensley and Penrith (1977) described a number of species that were established in Sandwich Bay (central Namib coast) outside of their normal biogeographic range. Donn and Cockroft (1989) studied the beginning of the recent replacement of the southern temperate fauna by the northern (sub-)tropical fauna at Bosluisbaai (northern Skeleton Coast, Namibia). Pether (1994) investigated past faunal communities in the unconsolidated sediments at depths of 120–140 m on the Orange shelf which accumulated during the post-glacial transgression. Around 14% of the detected bivalves are not typical members of the Namaqua Province molluscan fauna, but instead occur in the warm-temperate Algoa province of the Agulhas region. Therefore, Pether (1994) suggested warmer conditions in the Benguela area during the postglacial transgression (13.5–12.5 ka BP and 10 ka BP), with water advection from the Agulhas Current from the south and the Angola Current from the north resulting in a suppression of the upwelling system. He suggested that molluscs altered their ranges in response to changing oceanographic conditions, thereby resulting in a shift of the molluscan faunal provinces (Pether, 1994). West et al. (2004) described southward movements of the Angola-Benguela-Front (ABF) during the glacial maxima which enabled advection of the Angola Current into the Walvis Basin as indicated by tropical species in the associated sediments. Compton (2006), Compton (2007) investigated the sedimentary and faunal evolution of the pans of Bogenfels and Anichab (southern Namib coast). Both pans are located in the center of the upwelling area and are characterized in the present day by cool-temperate conditions. He described warm water molluscan faunas which recently occur in the warm, coastal waters of Angola. He also found the salinity tolerant clams *Gastrana matadoa* and *Solen capensis* which today are found in the warmer waters of the South African south coast (Kilburn and Rippey, 1982). Most recently, Heyns-Veale et al. (2022) analyzed the marine benthic mollusc ecoregions of South Africa following different statistical approaches and with a special emphasis on depth effects. Compton (2007) also characterized the foraminifera *Quinqueloculina* cf. *seminulum* as the dominant species in the sediments indicating warm and perhaps hypersaline conditions in the embayments. Compton (2006, Compton 2007) interpreted this fossil fauna to be associated with the mid-Holocene sea-level highstand.

Over the last 7000 years, sea-level fluctuations were subtle, moving less than 3 m over periods of hundreds of years at the southern African coast (see Miller et al., 1993; Miller et al., 1995; Baxter and Meadows, 1999; Compton, 2001; Compton, 2006; Compton, 2007; Cooper et al., 2018). The reconstruction of sea-level changes along the Namibian coastline is complicated by the fact that well preserved, datable, and unaltered sea-level index points are rare. The southern African high-energy coast is lacking in sheltered embayments with fine marine or lagoonal background deposits (Miller et al., 1995; Compton, 2006; Compton, 2007). Additionally, the coastal dune system of the Namib buried many earlier highstand deposits *via* active dune migration (Compton and Franceschini, 2005; Compton, 2006; Franceschini and Compton, 2006). However, some studies demonstrate the applicability of different sea-level index points to reconstruct past conditions. Compton (2007) described at Anichab Pan well-preserved mollusc assemblages as articulated shells in life position exposed on the pan surface. He also described north-south oriented ridges (yardangs) and valleys (yardang troughs) which developed during glacial lowstand by wind erosion (Compton, 2007).

The aim of this study is 1) to define temporal expansions of species-specific biogeographic ranges as indicators for variations in upwelling intensities by 2) dating and investigating the macrobenthic coastal communities from core material, following a latitudinal gradient when 3) analyzing the Holocene sedimentary evolution of (paleo-) lagoons along the Namibian coastline, and 4) to document biogenic records of regional Holocene sea-level fluctuation. Our results will complement existing datasets by documenting the sedimentary and faunal records of the lagoons along the Namibian coast in their function as

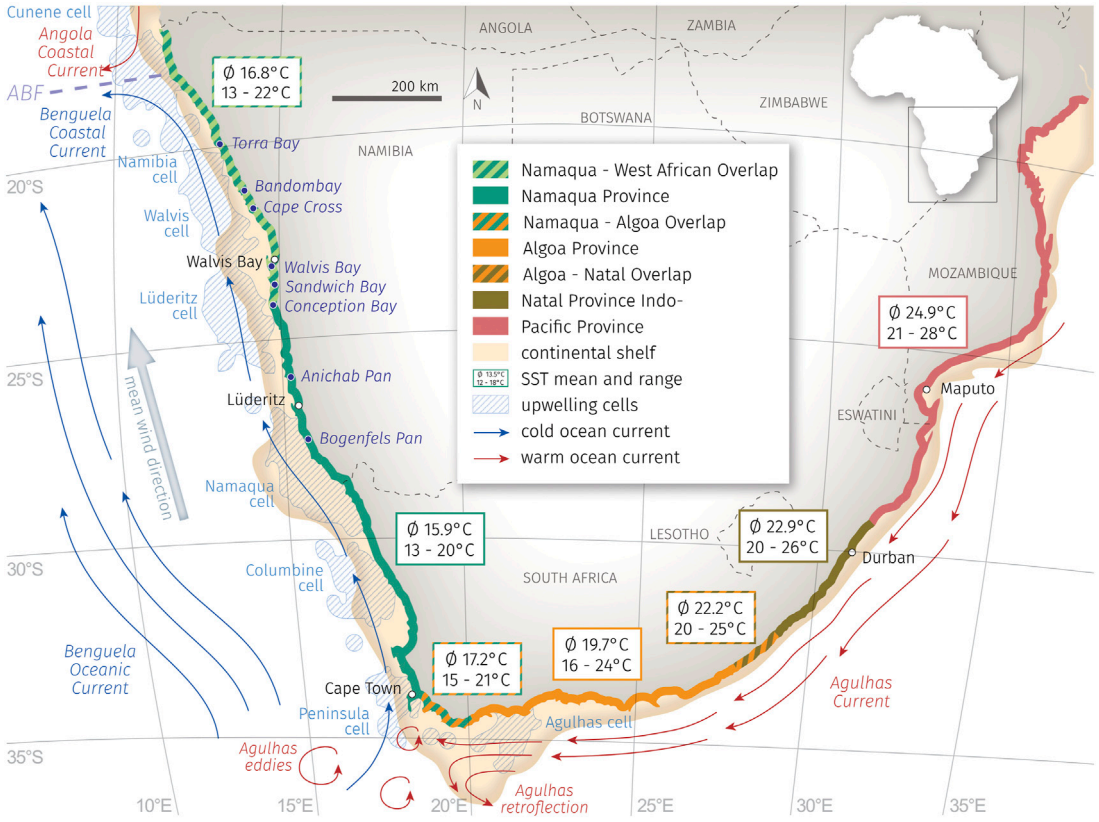

FIGURE 1
Location of studied (paleo-)lagoons (this study) and the coastal Anichab Pan (Compton, 2007) and Bogenfels Pan (Compton, 2006) in the context of the oceanographic situation around southern Africa with the warm water masses of Agul has Current and Angola Coastal Current (red) and the cool Benguela Current with the Benguela Coastal Current (both blue), the todays location of the Angola-Benguela-Front (ABF, violett), mean wind direction and resulting upwelling cells (light blue, hachured shapes, after Lutjeharms and Meeuwis, 1987). Marine biogeographic provinces/ecoregions along the southern African coastlines (modified after Kilburn and Rippey, 1982; Heyns-Veale et al., 2022) with coastal SST (mean and seasonal range, after CERSAT: http://cersat.ifremer.fr).

geoarchives preserving Holocene oceanic, environmental, and climatic signals.

2 Materials and methods

2.1 Regional setting

2.1.1 Benguela Upwelling System (BUS)

The atmospheric conditions along the Namibian coastline are characterized by the South Atlantic anticyclone with its southern longshore wind, which is relatively steady year-round and initiates a strong upwelling regime. Eight different upwelling cells have been described: the Cunene, Namibia, Walvis Bay, Lüderitz, Namaqua, Columbine, Peninsula, and Agulhas cells (Figure 1) (Lutjeharms and Meeuwis, 1987). Recently, the entire upwelling area has been restricted to the southwestern African coastline from the Angola-Benguela-Front near Cabo Frio (18.4°S) to the Agulhas Bank at Cape Agulhas (34.5°S) (Nelson and Hutchings, 1983; Summerhayes, 1983; Shannon, 1985; Boyd et al., 1987; Lutjeharms and Meeuwis, 1987; Hay and Brock, 1992; Dingle et al., 1996; Shannon and Nelson, 1996; Berger and Wefer, 2002; Baumann and Freitag, 2004; Leduc et al., 2010; Nicholson, 2010; Heinrich et al., 2011; Jury, 2017).

The upwelled nutrient-rich water (8–10°C) is transported northward *via* longshore drift and the north-directed Benguela Current. During active austral winter upwelling, the sea surface temperatures (SST) at the Namibian coast are around 12°C, whereas in austral summer they temporarily rise to 18°C with an annual mean temperature of 13.5°C (CERSAT).

Towards lower latitudes, the ABF separates the upwelling area from the water masses of the subtropical Angola current, which represents the southward-flowing extension of the south-equatorial countercurrent with SSTs of up to 27°C (Shannon et al., 1987; Hay and Brock, 1992). The ABF shows a seasonal

short-term variability in its N-S-extension from 10°S to 17°S (CERSAT). Sporadic, once-in-a-decade, extreme events occur in austral summer when the southward-flowing Angola Coastal Current reaches maximum latitudes as far south as 23°S (Moroshkin et al., 1970; Shannon et al., 1986). These events are described as "Benguela Niños" (Lass et al., 2000). The warm water intrusions lead to an SST increase of 2–8°C in the northern BUS (Emeis et al., 2009).

At the southern border, the upwelling system is bounded by a highly-variable frontal zone to the most southwesterly elongation of the retroflection zone of the Agulhas Current between 20°E and 16°E and 36°S and 38°S (Lutjeharms and van Ballegooyen, 1988; Shannon et al., 1989; Duncombe Rae, 1991; Summerhayes et al., 1995; Shannon and Nelson, 1996; Shannon, 2001; Baumann and Freitag, 2004; Emeis et al., 2009; Zhao et al., 2017). The Agulhas Current transports relatively warm, salty, and oligotrophic Indian Ocean surface water around the southern tip of Africa. At approximately 38°S south the Agulhas Current approaches the Subtropical Convergence (40°S) and most of the water reverses course back into the southern Indian Ocean, turning to the south-eastern direction and forming the Agulhas Retro Current (Hay and Brock, 1992; Shannon and Nelson, 1996; Zhao et al., 2017). Periodically, a small amount of the warm Agulhas Current water enters the southern Benguela region in the form of shedding large eddies (diameter <200 km) or by streams and plumes (Pether, 1994; Shannon and Nelson, 1996; Shannon, 2001; Baumann and Freitag, 2004; West et al., 2004; Emeis et al., 2009; Zhao et al., 2017). Different studies have indicated an increase in the Agulhas leakage during glacial-interglacial transitions which have in turn influenced the BUS by causing a positive density anomaly in the South Atlantic thus stimulating a stronger and more stable Atlantic meridional overturning circulation (for example Peeters et al., 2004; Martínez-Méndez et al., 2008, 2010; Dickson et al., 2010; Caley et al., 2014; Petrick et al., 2015).

2.1.2 Marine biogeographic provinces

The macrobenthic molluscan fauna of the southern African coastline has been divided into different marine provinces/ecoregions (see Kilburn and Rippey, 1982; Heyns-Veale et al., 2022). These biogeographical regions are categorized by characteristic faunal elements, but the boundaries between them are rather poorly defined with large overlapping zones (Figure 1). The authors described four different marine provinces: 1) the Namaqua/Southern Benguela Province, which includes most of the Atlantic coast from Cape Point to north of Lüderitz; 2) the Algoa/Agulhas Province from the Agulhas region to the Great Kei River mouth; 3) the Natal Province at the southeastern coast from the Umtata River to the Tugela River; and 4) the Indo-Pacific/Delagoa Province, which extends from the Tugela River across the tropical Indian Ocean.

The cool-temperate Namaqua Province is strongly influenced by the nutrient-rich and cold water of the Benguela current and local upwelling cells, with only a few sheltered bays and lagoons present along this extremely exposed coastline. It is characterized by giant kelp forests at and below the low-tide level. As is typical of cold waters, the Namaqua fauna is less diverse than in the warmer regions of the southeastern coast. According to Kilburn and Rippey (1982), the Anichab Pan and Bogenfels Pan belong to this marine province, but the borders to the northern Namaqua-West African Overlap are poorly defined due to insufficient knowledge of Namibian coastal fauna. The limited data from this area show a northward increase in the number of West African molluscs which have expanded from the Angolan coast. The southern border of the Namaqua Province is categorized as the Namaqua-Algoa Overlap, a transition zone where Atlantic and Agulhas waters mix. Faunal elements of both Namaqua Province and Algoa Province occur in this region without a sharp discontinuity. The Algoa Province is characterized by a high percentage (>70%) of warm-temperate endemic molluscs, some of them belonging to the Indo-Pacific and subtropical Natal endemics which reach their range limits at this point. They are limited by cold upwelling waters, mainly during austral winter, whereas cold water species are repressed by higher austral summer temperatures. To the east, the location of the Algoa-Natal Overlap is poorly defined even if the existence of a transitional zone between both marine provinces is accepted.

All investigated lagoons of this study belong to the province of the Namaqua-West African Overlap with Conception Bay located at the southern rim to the Namaqua Province.

2.1.3 Study sites

Coastal lagoons and related pans are a common morphological feature occurring along the entire south-western coastline from South Africa to Namibia and Angola and reflecting the regional wind and wave regime. The semi-diurnal tide at Walvis Bay has a mean range of 1.42 m at spring tide (1.9 m at equinoxes) and 0.62 m at neap tide (Wearne and Underhill, 2005). The coastal environment can be classified as high-energy, swell-dominated with a pronounced northward-directed longshore transport.

The formation of coastal lagoons begins with the initiation of a sand spit at headlands or river mouths due to significant longshore sediment transport. Later, lagoons with tidal channels, tidal flats, and salt marshes develop protected by the sand spit barrier from high wave energy (Buzer and Sym, 1983). The lagoons experienced periodic flooding by tides and extreme high waters. Under sheltered depositional conditions the lagoons are successively filled with sediment, which leads to the formation of a paleolagoon (synonymously termed coastal pan). Som2e coastal lagoons and pans have a connection to groundwater which can occur and seep

TABLE 1 Characteristics of the studied (paleo-)lagoons and drilling sites along the Namibian coast.

Lagoon/pan	Conception Bay					Sandwich Bay					Shell midden
Core Nr.	D1	D2	D3	D4	D5	D5	D6	D7	D1/D2	D3/D4	—
Coordinates	S24° 6.603	S24° 1.444	S24° 1.428	S23° 56.094	S23° 55.776	S23° 32.046	S23° 28.063	S23° 24.295	S23° 21.974	S23° 21.966	~ S23° 21.000
(WGS 84)	E014° 30.145	E014° 32.935	E014° 32.841	E014° 30.876	E014° 30.804	E014° 29.112	E014° 28.769	E014° 28.822	E014° 29.889	E014° 29.861	~ E014° 30.000
Core height	2.0 m aMSL	0.8 m aMSL	1.0 m aMSL	1.6 m aMSL	2.1 m aMSL	3 m aMSL	2 m aMSL	2 m aMSL	5.2 m aMSL	4.2 m aMSL	10 m aMSL
Core depth	150 cm	74 cm	113 cm	142 cm	140 cm	203 cm	148 cm	163 cm	D1: 144 cm	D3: 131 cm	shell midden
									D2: 144 cm	D4: 105 cm	at surface
Calibrated ^{14}C ages [cal yr BP (2σ range)]	0–2 cm:	19 cm:	0–4 cm:	*Donax serra* (surface):	75 cm:	0–3 cm:			D1 - 92–98 cm:	D3 - 50–54 cm:	*Austromegabalanus*
	1448 (1633–1277)	802 (971–637)*	295 (473–95)*		174 (336-0)*	5094 (5336–4823)			466 (621–300)	132 (280-0)*	*cylindricus*
	120 cm:	60 cm:	15–19 cm:	161 (315-0)*		72–77 cm:			D2 - 57–64 cm:	D4 - 10 cm:	115 (263-0)*
	2816 (3030–2631)	911 (1103–721)	376 (531–195)*	113–118 cm:		4694 (5007–4394)			111 (260-0)*	174 (336-0)*	*Parechinus*
			18 cm:	226 (419–28)*		77 cm:			D2 - 78 cm:	D4 - 29 cm:	*angulosus*
			360 (514–163)*	130–137 cm:		5740 (5934–5547)*			125 (272-0)*	97 (247-0)*	187 (357-0)*
			112 cm:	243 (436–45)*		162 cm:			D2 - 103 cm:	D4 - 42 cm:	
			1261 (1439–1065)*			3251 (3449–3029)*			102 (252-0)*	102 (252-0)*	
									D4 - 86–89cm:		
									564 (712–416)		
									D4 - 90 cm:		
									129 (276-0)*		

Lagoon/pan	Peat	Walvis Bay			Cape Cross		Bandombay			Torra Bay
Core Nr.	—	D3/D4	D5/D6	D1/D2	D2	D1	D1	D2/D3	D4/D5	D1
Coordinates	S23° 17.652	S23° 12.418	S23° 05.492	S22° 57.115	S21° 46.344	S21° 46.138	S21° 22.081	S21° 21.854	S21° 21.833	S20° 22.355
(WGS 84)	E14° 29.720	E014° 28.332	E014° 27.064	E014° 25.615	E013° 57.784	E013° 57.876	E013° 45.755	E013° 45.616	E013° 45.619	E013° 16.759
Core height	0 m aMSL	2.6 m aMSL	4.0 m aMSL	4.4 m aMSL	1.9 m aMSL	2.0 m aMSL	3.7 m aMSL	4.8 m aMSL	4.3 m aMSL	0.3 m aMSL
Core depth	outcrop	D3: 136 cm	D5: 97 cm	D1: 127 cm	203 cm	192 cm	240 cm	D2: 49 cm	D4: 50 cm	D1: 224 cm
	(50 cm)	D4: 140 cm	D6: 93 cm	D2: 118 cm				D3: 55 cm	D5: 50 cm	D2: 245 cm
Calibrated ^{14}C ages [cal yr BP (2σ range)]	surface:	D3 - 35–40 cm:	D6 - 4–6 cm:	D2 - 4–8 cm:	12–14 cm:	54–60 cm:	175–190 cm:	D3 - 30–35 cm:		50–60 cm:
	733 (772–677)	2396 (2671–2142)	389 (452–347)	522 (662–357)	4916 (5199–4689)*	5040 (5272–4830)*	6004 (6257–5745)	571 (718–425)		5423 (5588–5297)

(Continued on following page)

near the

10.3389/feart.2022.898843

TABLE 1 (*Continued*) Characteristics of the studied (paleo-)lagoons and drilling sites along the Namibian coast.

Lagoon/pan	Peat	Walvis Bay			Cape Cross		Bandombay	Torra Bay
	50 cm: 1341 (1377–1302)	D3 - 60–70 cm: 3409 (3635–3180)	D6 - 78–81 cm: 1709 (1951–1690)	D2 - 60–65 cm: 2482 (2712–2282)	106.5–107.5 cm: 5177 (5424–4942)* 139–144 cm: 5279 (5484–5027)*	87 cm: 5136 (5345–4872)* 100–112 cm: 6109 (6304–5895) 115 cm: 5053 (5279–4837)* 121 cm: 5203 (5438–4964)* 140 cm: 5136 (5345–4872)* 148 cm: 5136 (5345–4872)* 149 cm: 5236 (5460–4982)* 152–155 cm: 5183 (5428–4949)*		170–176 cm: 5598 (5763–5440)

*^{14}C dating on shell material.

10.3389/feart.2022.898843

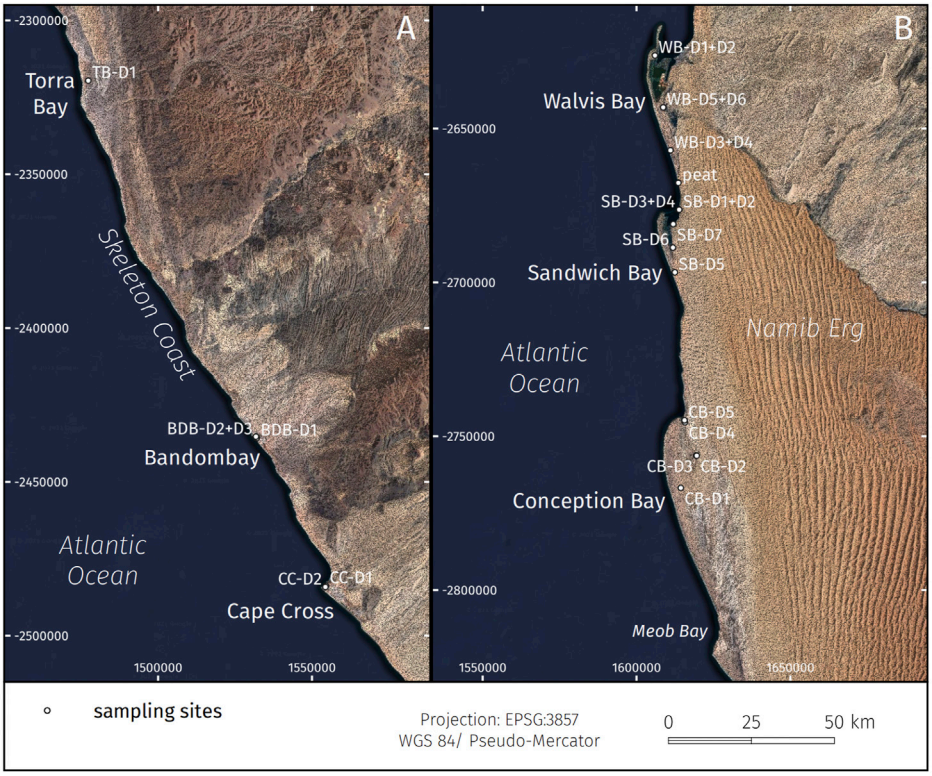

FIGURE 2
(A) Northern and **(B)** southern coastal study areas with investigated (paleo-)lagoons of the Namibian coastline with associated sampling sites (black dots, TB = Torra Bay, BDB = Bandombay, CC = Cape Cross, WB = Walvis Bay, SB = Sandwich Bay, CB = Conception Bay). Topographic data generated from SRTM-model (Farr et al., 2007), satellite data by SIO, NOAA, U.S. Navy, NGA, GEBCO, satellite image by Google, Landsat/Copernicus.

surface. During phases of lower sea level, the pans are affected by deflation and mobile eolian dune ridges as well. Wind erosion also forms north-south-oriented bedrock ridges (yardangs) and valleys (yardang troughs) (Compton, 2007).

The studied lagoons and coastal pans stretch along the coast between 24°25'S in the south (Conception Bay) up to 20°20'S in the north (Torra Bay). In total, six coastal lagoons and their related pans have been investigated, namely, Conception Bay, Sandwich Bay (23°27'S), Walvis Bay (23°05'S), Cape Cross (21°48'S), Bandombay (21°22'S), and Torra Bay. Only Sandwich Bay and Walvis Bay possess active lagoons whereas the others have completely been transformed into paleolagoons or coastal pans. Walvis Bay has remained a wide-open lagoon whereas Sandwich Bay is largely silted up with only shallow waters and highly dynamic sand spit at the lagoon inlet in the north. Conception Bay is flooded in parts during high tides, but does not contain an active lagoonal area. Cape Cross has small, episodically flooded pools at the southern end of the pan behind the sand barrier. Flooding is caused by two different processes: *via* continuous seawater seepage through the sand spit or by water washed over the sand barrier during extreme high tides or storm events. The pans of Bandombay and Torra Bay are mainly dry and do not have any open expanse of water.

The areas of the lagoons and pans differ, with Conception Bay as the largest pan (surface area >900 km^2) followed by Walvis Bay with around 260 km^2 (pan area ~92 km^2, lagoon ~167 km^2), Sandwich Bay with 49 km^2 (pan area ~13 km^2, lagoon ~36 km^2), Cape Cross 45 km^2, Bandombay (in the investigated part) 12 km^2, and Torra Bay 32.5 km^2.

2.2 Sediment cores

In total, 26 sediment cores were taken in September 2014 and March 2015 with a vibro-coring system (Wacker Neuson IE high-frequency vibrator head and generator) and aluminum tubes of 80 mm diameter (Table 1). The sediment cores reached a maximum length of 245 cm (Torra Bay). The sampled lagoons and pans were chosen along the SSE-NNW-directed coastline from 24°07'S (Conception Bay) to 20°22'S (Torra Bay) to document the latitudinal gradient along the Namibian coast towards the today's location of the ABF at ~17°S. Within the coastal lagoons and paleolagoons,

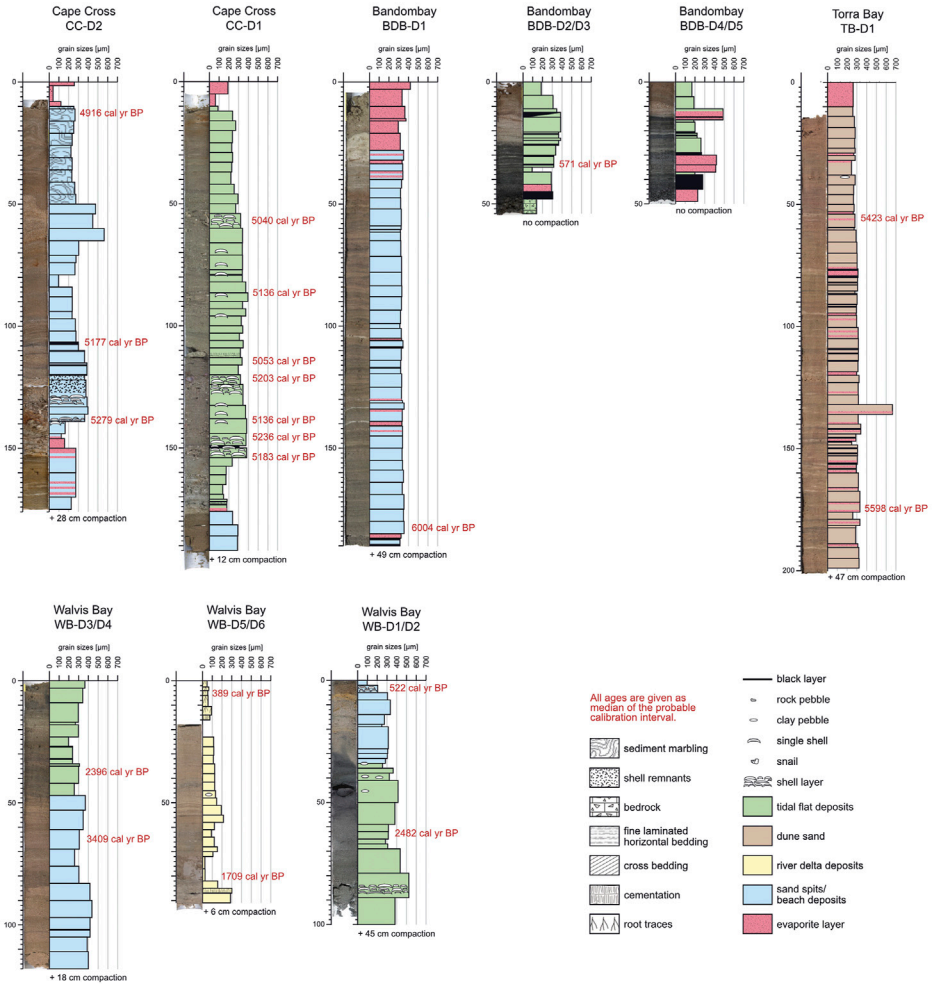

FIGURE 3
Photos and logs of the sediment cores investigated in the northern (paleo-)lagoons (Torra Bay, Bandombay, Cape Cross, Walvis Bay) with an illustration of the mean grain sizes (per sampling interval), calibrated ^{14}C ages (given as median probability, for 2σ intervals see Supplementary Table S4), faunal remnants, and primary as well as secondary sedimentary structures.

N-S-directed transects were sampled following successive silting-up processes (Figure 2). In Torra Bay, only one sediment core was taken at the rim due to the inaccessible soft surface of the pan. Core splitting, sediment/fauna sampling, and documentation were conducted at the drilling locations without longer transport of the cores. The sediment color was directly determined using the Munsell soil color chart after splitting the cores into halves.

2.2.1 Grain size analyses

For grain size analyses in the laboratory, all subsamples were treated with H_2O_2 (35%) and HCl (25%) to dissolve particulate organic matter and carbonate. Additionally, all samples were treated with $(KPO_3)_n$ for 8–12 h to prevent coagulation of clay particles. Sediment particle sizes were analyzed as a suspension from three replicates with a Horiba Scattering Particle Size Distribution Analyzer LA-950. Grain size distribution is given for 92 size classes between 0 µm and 2,000 µm.

2.2.2 Radiocarbon dating

^{14}C age dates were preferably determined from shell material of different core depths if possible double valved (articulated) bivalves. Where no shell material was present the ^{14}C content of organic carbon in the sediment was measured. The AMS ^{14}C measurements and calibrations were performed in the AMS ^{14}C Laboratory of Poznań University (Poland). Methods of chemical pre-treatment generally followed those used in the Oxford Radiocarbon Accelerator Unit as described by Brock et al. (2010). A total of 40 shell samples and 23 sediment samples were dated. The calibration of all ^{14}C ages was performed

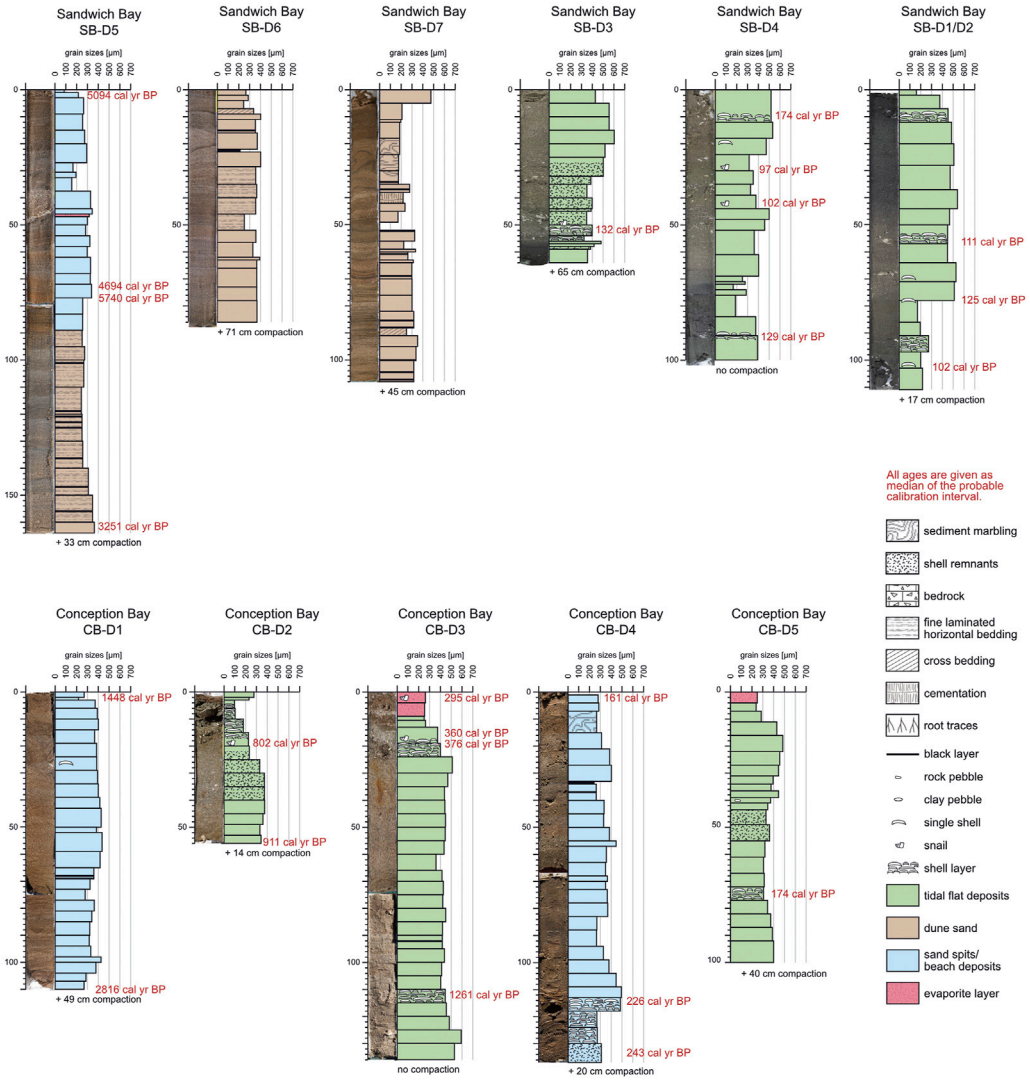

FIGURE 4
Photos and logs of the sediment cores investigated in the southern (paleo-)lagoons (Sandwich Bay, Conception Bay) with an illustration of the mean grain sizes (per sampling interval), calibrated ^{14}C ages (given as median probability, for 2σ intervals see Supplementary Table S4), faunal remnants, and primary as well as secondary sedimentary structures.

using the Calib Rev. 8.2 (http://calib.org/calib/calib.html). All shell samples and tidal flat samples were calibrated with the Marine20 calibration curve (Heaton et al., 2020), all terrestrial sediment samples with the Southern Hemispheric SHCal20 calibration curve (Hogg et al., 2020). Sediment samples of the sand spits were estimated to be 95% of marine origin and only 5% of terrestrial and were therefore calibrated with both calibration curves (mixing ratio 95/5). For reservoir correction of all marine samples a ΔR value of −1 ± 59 years was used representing the mean of the five nearest regional positions with published ΔR values (Dewar et al., 2012). All calibrated age data are given as median probability with a 2σ error interval (see Supplementary Table S4).

2.2.3 Biogeographic analyses

For biogeographic and ecologic analyses, shell material was sampled from the sediment cores, fossil pan surfaces, shell middens and nearby beaches (recent surface). All biogenic remnants were determined after Kilburn and Rippey (1982), Branch et al. (1994), and Ardovini and Cossignani (2004) down to the species level. Taxonomic species names were cross-referenced using the World Register of Marine Species (WoRMS 2022). The marine biogeographic provinces/ecoregions along the southern African coastlines follows Kilburn and Rippey (1982) and Heyns-Veale et al. (2022).

2.2.4 Sea-level index points

For those datasets used for the regional relative mean sea-level curve, we followed the HOLSEA workflow (Hijma et al., 2015; Khan et al., 2019, Supplementary Table S1 of this study) to ensure a standardized handling of sea-level index points, mainly with respect to their vertical error. All uncertainties of a respective datum were processed after inserting the relevant data into the 77 column comprehending sea-level spreadsheet of Khan et al. (2019, Supplementary Data available online at https://doi.org/10.1016/j.quascirev.2019.07.016). Height information for all sampling sites (see Table 1) was derived from datasets of the SRTM-Model (Farr et al., 2007) and from daily calibrated DGPS measurements. Additionally, we summarized the requisite background information regarding the indicative meanings of the different mollusc and peat samples in a separate table (see Supplementary Table S2 this study).

3 Results

3.1 Sedimentary facies

The Namibian coastal lagoons and their related pans revealed four different depositional sub-environments that can also be distinguished as sedimentary facies in the Holocene sediment cores (see Figures 3, 4 for details regarding sedimentary structures, mean grain size, and color). The four facies reflect the principle modern sedimentary units of this specific coastal depositional environment, namely the sand spit/beach facies, the tidal flat facies of the active lagoon, the evaporitic pan facies, and the eolian dune facies. Additionally, a river delta facies can be defined in cores taken in the paleomouth of the ephemeral Kuiseb River. All depositional processes are indicative of the respective facies and can be observed contemporaneously in the field.

3.1.1 Sand spit/beach facies

Diagnostic features: This facies occurs in cores from all studied (paleo-)lagoons except Torra Bay, where only one core was taken in a relatively landward position. The sand spit/beach facies consists of medium-grained brown to yellowish-brown sand (quartz, feldspars, pyroxenes) with varying amounts of biogenic carbonate debris and mollusc shells. Sedimentary structures are dominated by horizontal to slightly oblique laminated bedding partly showing low-angle disconformities.

Depositional processes: Due to the wave-dominated character, swash and backwash is the most prominent sedimentary process. During extraordinarily high waters and storm surges the sand spits are affected by washovers causing sediment fans with steeper foresets on the backside of the sand spits. In phases with a dry sediment surface, eolian sediment transport causes wind ripples, small dunes, deflation, and shell lags mainly on top of the sand spits. Bioturbation is low to absent.

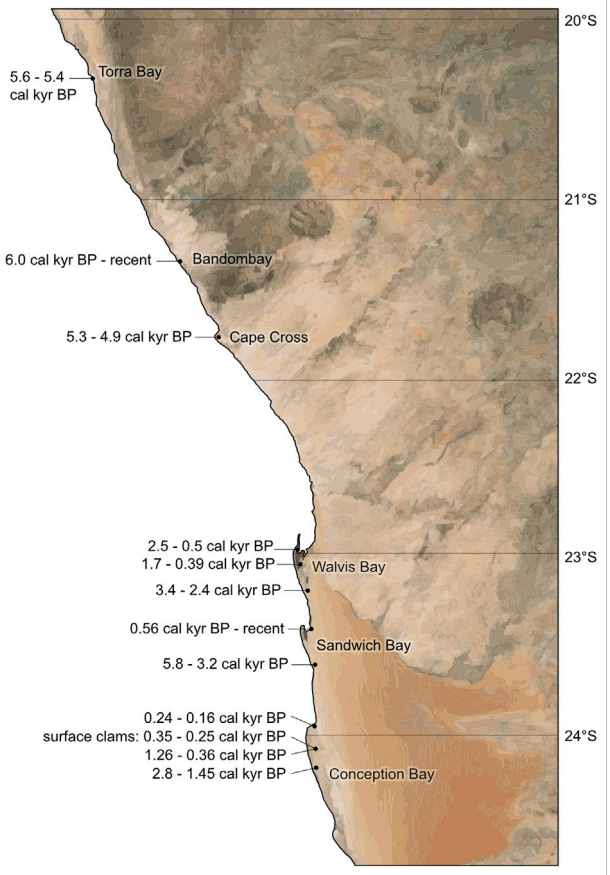

FIGURE 5
Spatial distribution of the calibrated ^{14}C AMS age datings. Measurements were done on shell material and content of organic carbon in the core sediments and surface samples along the Namibian coast from Conception Bay in the south to Torra Bay in the north.

3.1.2 Tidal flat facies

Diagnostic features: Similar to the sand spit/beach facies, the tidal flat facies is found in cores from all (paleo-)lagoons except Torra Bay. The mean grain sizes cover a broad range from very fine sand to coarse sand. However, most of the dark grey to greyish-brown sediment belongs to the medium sand fraction. Shell debris, thick shell layers, and articulated shells in life position are common within the tidal flat facies. Rarely, isolated pebbles occur. Horizontal bedding, even lamination, and small-scale cross-bedding are typical sedimentary structures. In some cores, dark grey to black colors indicate fine-grained organic-rich layers and microbial mats.

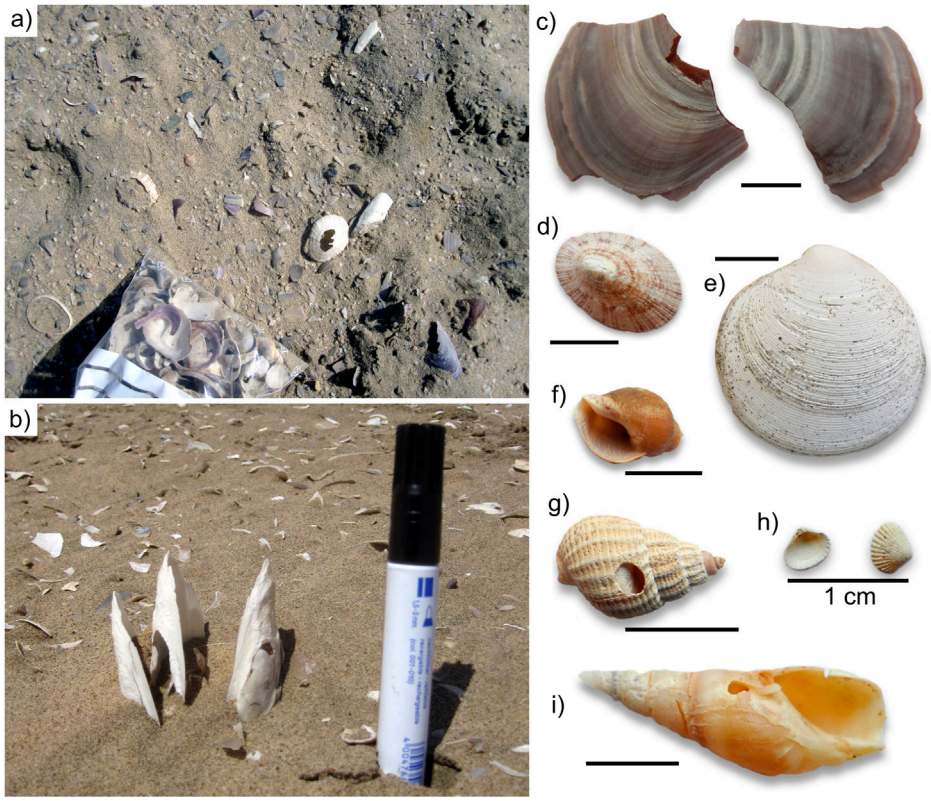

FIGURE 6
(A) Shell midden at Sandwich Bay; **(B)** fossil double-valved (articulated) clams *Lutraria in situ* at the pan surface of Conception Bay; shells which illustrate the highly diverse cool to warm temperate to subtropical fauna at the Namibian coastline: **(C)** *Choromytilus meridionalis*, **(D)** *Helcion dunkeri*, **(E)** *Dosinia lupinus*, **(F)** *Nucella dubia*, **(G)** *Nassarius niveus*, **(H)** *Carditopsis rugosa*, **(I)** *Bullia digitalis*.

Depositional processes: The tidal flat facies reflects deposition in a sheltered lagoonal environment in the back of the sand spit barrier. The broad range in grain sizes is caused by temporal and spatial small-scale hydrodynamic variations. The thick shell layers are mainly related to lateral migration of tidal channels within the lagoon, terminating in a tidal inlet which can temporarily be closed due to growth or lateral migration of the sand spit or due to decrease of the tidal prism. When silted up above the high-water level, typical salt marsh vegetation begins to grow on top of the tidal flat surface. This is restricted to places in the lagoon with brackish conditions due to groundwater seepage. Bioturbation is variable.

3.1.3 Evaporitic pan facies

Diagnostic features: Layers of up to 30 cm-thick light grey to brownish-grey evaporites frequently occur on top of the recent sediment surface. In the northernmost paleolagoons of our study area, namely, Cape Cross, Bandombay, and Torra Bay, thin evaporite layers can also be found in the deeper parts of the cores intercalated in all types of sediment facies. The evaporite layers mainly consist of salt (halite), gypsum and carbonates. Gypsum also occurs as gravel-size idiomorphic crystals within the sand matrix.

Depositional processes: This facies is restricted to the sheltered inner part of the (paleo-)lagoon where seepage ground-/porewater evaporates under the semi- to hyper-arid climatic conditions and leads to the pan-like character of the lagoons. Additionally, the surficial evaporite crust prevents the sediment surface from deflation. In contrast, modern pan surfaces are frequently buried by eolian-transported sand sheets (higher wind speeds) or dunes (low to moderate wind speeds) as represented by the eolian dune facies.

3.1.4 Eolian dune facies

Diagnostic features: The mean grain size of the eolian dune facies has a relatively narrow range at the transition

TABLE 2 List of macrobenthic faunal species from the sampled (paleo-)lagoons, beaches, and shell midden, blue: recently occurring in study area; orange: recently not occurring. Biogeographic ranges after Kilburn and Rippey (1982), Branch et al. (1994), World Register of Marine Species (WoRMS, 2022) and Ocean Biodiversity Information System (OBIS, 2022).

		Namaqua -West African Overlap	Namaqua Province	Namaqua - Algoa Overlap	Algoa Province	Algoa - Natal Overlap	Natal Province	Indo-Pacific Province
Torra Bay	*Argobuccinum pustulosum*	2	1/2/3	1/2/3	1/2/3	1/2/3		
	Burnupena lagenaria		1/2/3	1/2/3	1/2/3	1/2/3	1/2/3	
	Choromytilus meridionalis	2/3	1/2/3	1/3	1/3	3		
	Chthamalus dentatus	3	1/3	1/3	1/3	1/3	1/3	1/3
	Cymbula miniata	2/3	1/2/3	1/2/3	1/2/3	1/2/3	3	
	Cymbula safiana	2/3						
	Discinisca tenuis	1/3	1/3					
	Perna perna	1/2/3	1/2/3	1/2/3	1/2/3	1/2/3	1/2/3	1/2/3
	Scutellastra argenvillei	2/3	1/2/3	1/2/3	1/2/3	1/2/3	1/3	3
	Stramonita haemastoma	1/3	3					
Cape Cross	*Argobuccinum pustulosum*	2	1/2/3	1/2/3	1/2/3	1/2/3		
	Assiminea ovata		3	3	1/2/3	1/2/3	1/2/3	1/2/3
	Bullia digitalis	1/2/3	1/2/3	1/2/3	1/2/3	1/2/3	1/3	
	Bullia tenuis			2/3	2/3	2/3	2/3	2/3
	Burnupena lagenaria		1/2/3	1/2/3	1/2/3	1/2/3	1/2/3	
	Choromytilus meridionalis	2/3	1/2/3	1/3	1/3	3		
	Discinisca tenuis	1/3	1/3					
	Donax serra	1/2/3	1/2/3	1/2/3	1/2/3	1/2/3	1/3	
	Dosinia orbignyi	1/2	1/2/3	1/2	1/2	1/2		
	Loripes clausus				1/2/3	1/2/3	1/2/3	1/2/3
	Lugubrilaria lugubris		1/2/3	1/2/3	2	2	2	
	Moerella tulipa		3	1/2/3	1/2/3	1/2/3		
	Nassarius niveus	1/2/3	1/2/3	3	3			
	Nucella dubia	2/3	1/2/3	1/2/3	1/2/3	1/2/3	1/2	
	Nucella squamosa	2/3	1/2/3	1/2/3	1/2/3	1/2/3	1/2	
	Perna perna	1/2/3	1/2/3	1/2/3	1/2/3	1/2/3	1/2/3	1/2/3
	Stramonita haemastoma	1/3	3					
	Venerupis corrugata	1/2	1/2/3	1/2/3	1/2/3	1/2	1/2	
Walvis Bay	*Donax serra*	1/2/3	1/2/3	1/2/3	1/2/3	1/2/3	1/3	
Sandwich Bay	*Amphibalanus amphitrite*	3		1	1/3	1/3	1/3	1/3
	Aulacomya atra	1/3	1/3	1/3	1/3	1		
	Austromegabalanus cylindricus		1/3	1	1			
	Choromytilus meridionalis	2/3	1/2/3	1/3	1/3	3		
	Donax serra	1/2/3	1/2/3	1/2/3	1/2/3	1/2/3	1/3	
	Dosinia orbignyi	1/2	1/2/3	1/2	1/2	1/2		
	Hiatula capensis			1	1/2/3	1/2	1	
	Nassarius niveus	1/2/3	1/2/3	3	3			
	Parechinus angulosus		1/3	1/3	1/3	1/3	1	
	Venerupis corrugata	1/2	1/2/3	1/2/3	1/2/3	1/2	1/2	

(Continued on following page)

TABLE 2 (*Continued*) List of macrobenthic faunal species from the sampled (paleo-)lagoons, beaches, and shell midden, blue: recently occurring in study area; orange: recently not occurring. Biogeographic ranges after Kilburn and Rippey (1982), Branch et al. (1994), World Register of Marine Species (WoRMS, 2022) and Ocean Biodiversity Information System (OBIS, 2022).

		Namaqua -West African Overlap	Namaqua Province	Namaqua - Algoa Overlap	Algoa Province	Algoa - Natal Overlap	Natal Province	Indo-Pacific Province
Conception Bay	*Argobuccinum pustulosum*	2	1/2/3	1/2/3	1/2/3	1/2/3		
	Aulacomya atra	1/3	1/3	1/3	1/3	1		
	Bullia digitalis	1/2/3	1/2/3	1/2/3	1/2/3	1/2/3	1/3	
	Bullia laevissima	1/2/3	1/2/3	1/2/3	1/2/3	1/2/3	1	
	Burnupena lagenaria		1/2/3	1/2/3	1/2/3	1/2/3	1/2/3	
	Burnupena papyracea	2	1/2/3	1/2/3	3	3	3	
	Carditopsis rugosa			3	1/2/3	1/2/3	1/2/3	
	Choromytilus meridionalis	2/3	1/2/3	1/3	1/3	3		
	Cymbula compressa	2/3	1/2/3	2/3	2/3			
	Cymbula miniata	2/3	1/2/3	1/2/3	1/2/3	1/2/3	3	
	Donax serra	1/2/3	1/2/3	1/2/3	1/2/3	1/2/3	1/3	
	Dosinia orbignyi	1/2	1/2/3	1/2	1/2	1/2		
	Gibbula cicer	1/2	1/2/3	1/2/3	1/2/3	1/2/3	1/3	
	Helcion dunkeri	1/2/3	1/2/3	1/2/3	1/2/3	1/2/3	1/2/3	
	Homalina trilatera	3	1/2/3	1/2/3	1/2/3	1/2/3	1/3	3
	Limaria tuberculata			3	3			
	Linatella caudata	2	1/2	1/2	1/2	1/2	1/2/3	1/2/3
	Loripes clausus				1/2/3	1/2/3	1/2/3	1/2/3
	Lugubrilaria lugubris		1/2/3	1/2/3	2	2	2	
	Lutraria lutraria	1	1/2/3	1/2/3	1/2/3	1/2		
	Mactra glabrata	2	1/2/3	1/2/3	1/2/3	1/2/3	1	1
	Nassarius niveus	1/2/3	1/2/3	3	3			
	Notomegabalanus algicola	1/3	1/3	1/3	1/3	1/3	1	
	Nucella squamosa	2/3	1/2/3	1/2/3	1/2/3	1/2/3	1/2	
	Pallidea palliderosea			1/2/3	1/2/3	1/2		
	Prunum capense	2	1/2/3	2/3				
	Scutellastra argenvillei	2/3	1/2/3	1/2/3	1/2/3	1/2/3	1/3	3
	Scuttelastra barbara		1/3	1/3	1/3	1/3	1/3	3
	Siphonaria capensis	3	1/3	1/3	1/3	1/3	1/3	1
	Striostrea margaritacea		3	1/2/3	1/2/3	1/2/3	1/2/3	1/2/3
	Tectonatica tecta	1/2	1/2/3	1/2/3	1/2/3	1/2		
	Trochita trochiformis	3						
	Turritella capensis		1/2/3	1/2/3	1/2/3	1/2		
	Venerupis corrugata	1/2	1/2/3	1/2/3	1/2/3	1/2	1/2	

1) Branch et al. (1994), 2) Kilburn and Rippey (1982), 3) WoRMS (2021) and OBIS (2021)

from fine to medium sand. The grain shape is subangular to subrounded and the sediment color is brown to yellowish or reddish brown. The most frequently-occurring sedimentary structures are finely-laminated planar horizontal bedding (wind-blown sand sheets) or low angle-dipping cross-bedding at both small and large scales (ripples to dunes). While quartz serves as the main lithoclastic component, the sediment is also composed of heavy minerals as well as biogenic carbonate debris.

Depositional processes: The semi- to hyper-arid climatic conditions and the lack of sediment-stabilizing vegetation favors eolian sediment transport in most regions along the Namibian coast, which possesses the largest and most extensive coastal dune complex in the world. The aeolian material has its

source in the catchment of the Orange River. From the mouth it is distributed onshore by northward directed longshore currents. At some places, where the coastline orientation changes, the feldspatho-quartzose sand (Garzanti et al., 2014) is blow landward along distinct sand pathways (Spaggiari et al., 2006). Remote sensing time series have shown that the eolian dune facies represents the most dynamic facies type. In the south, where the Namib Sand Sea directly borders the Atlantic coastline, the feet of large eolian dunes directly end in the lagoons. Additionally, smaller dunes, partly occurring in isolation or as dune fields are formed on the dry paleolagoon (pan) surface or on the sand spit migrating downwind.

3.1.5 River delta facies

Diagnostic features: The fluvial sediment differs strongly from those of the lagoon-related facies types in both composition of the lithoclastic material and the grain size distribution. The sediment consists of quartz frequently enriched with varying amounts of feldspar and mica (mainly biotite) resulting in a manifold alternation of brighter (greyish brown to yellowish brown) and darker (dark brown to dark grey) mm-thick horizontal layers. At some depth distinct and several cm-thick clay layers are found. Reworked clay layers occur as pebbles in the upper portion. The grain size ranges from clay to medium sand with the average size in the very fine to fine sand fraction. Root traces can frequently be observed and are caused by the shrubby vegetation present in the river delta. Shells or shell fragments indicating a marine influence are missing.

Depositional processes: This facies is restricted to the innermost southeastern part of the Walvis Bay lagoon which also inhabits the (paleo-)mouth of the ephemeral Kuiseb River. Mineral composition reveals 1) a source area corresponding to the upper catchment of the Kuiseb River where rocks of the Kuiseb formation (mainly represented by mica schists and quartzites) are outcropping, and 2) an episodic sediment transport over shorter distances.

3.2 Age determination

In total, 63 samples (shell material and sediment) were analyzed to obtain ^{14}C ages. Seven samples (six from shell material of Sandwich Bay and one evaporite crust from Bandombay) were too young to produce evaluable ages and were rejected from the presented results. From the 56 usable results, 34 results were measured from shell material and 22 were determined from carbon-rich sediment layers (for details see Figures 3, 4). The shells originate from sediment cores as well as from pan surfaces, a shell midden at Sandwich Bay (two samples, *Austromegabalanus cylindricus* and *Parechinus angulosus*), double-valved (articulated) clams in life-position at the pan surface of Conception Bay (two samples *Lutraria lutraria*) and from the sediment surface directly at the location of D4 in Conception Bay (one sample *Donax serra*).

All age determinations revealed a clustering into different time intervals: 6.0–4.7 cal kyr BP, 3.4–2.4 cal kyr BP, 1.7 cal kyr BP, 1.4–1.3 cal kyr BP, 0.9–0.7 cal yr BP, and 0.6–0.1 cal kyr BP.

Generally, the sediment cores show a regular stratigraphic order with younger ages closer to the pan surfaces. There are two outliers with divergent ages that we also rejected from our analysis. In the sediment core CC-D1 (Cape Cross) the sediment sample from 100–112 cm revealed a ^{14}C age of 6.1 cal kyr BP but all surrounding shell samples presented an age of 5.1 cal kyr BP. In the core SB-D5 (Sandwich Bay), the lowermost sample (162 cm) was dated with an age of 3.3 cal kyr BP, but all overlying sediment samples presented ages from 5.7 cal kyr BP to 4.7 cal kyr BP. However, most sediment cores do not contain sediment sequences covering long time intervals, but rather shorter time slices of up to a maximum of 2.0 kyr and mainly of several hundred years. One exception is the long sediment core of Bandombay (BDB-D1) which contains sediments of a 6.1 kyr interval.

Inside the same coastal lagoon or pan, the different sediment cores cover ages, which as a whole, decrease towards the northern direction. This reflects the expected successive silting-up and filling in this regional context (Figure 5). The following time periods are covered inside the single (paleo-)lagoons: Conception Bay: 2.8–0.2 cal kyr BP, Sandwich Bay: 5.7–0.1 cal kyr BP, Walvis Bay: 3.4–0.4 cal kyr BP, Cape Cross: 5.3–4.9 cal kyr BP, Bandombay: 6.0-recent cal kyr BP and Torra Bay: 5.6–5.4 cal kyr BP.

3.3 Biogeographic analyses

The macrobenthic fauna remnants for the biogeographic analyseswere collected from the sediment cores of four (paleo-)lagoons (Conception Bay, Sandwich Bay, Cape Cross, Torra Bay) as well as from dry pan surfaces near the core locations and along nearby beaches, including a ~200-year-old shell midden at Sandwich Bay (Figure 6).

In total, 221 samples were collected from sediment cores, pan surfaces, and from recent beaches. Identifiable shells were sampled in Conception Bay, Sandwich Bay, Walvis Bay, Cape Cross, and Torra Bay. No shell material was sampled in Bandombay.

It was possible to identify 46 different macrobenthic species from several regional biogeographic provinces/ecoregions (Table 2). Most of the fauna are commonly found in the majority of the recent cool-to-warm temperate provinces (see also Figure 1). Some sampled species, for example, *Cymbula safiana, Discinisca tenuis, Stramonita haemastoma*, and *Trochita trochiformis* occur exclusively in the Namaqua-West African Overlap (and further north), which is the regional province of the study area where all

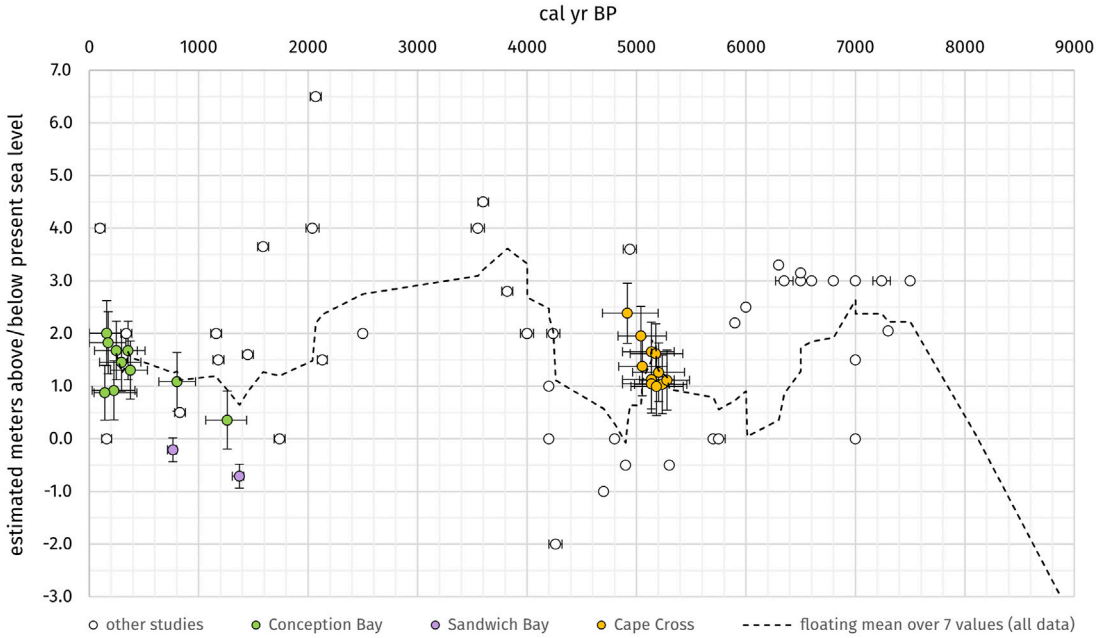

FIGURE 7
Sea-level data points from this study and other studies (white circles): Conception Bay (green), Sandwich Bay/Walvis Bay (violet) and Cape Cross (orange). The black graph is the floating mean over 7 values of all shown datasets and approximately visualizes the estimated late to mid-Holocene sea-level fluctuations along the southwestern African coast.

investigated pans are located. In contrast, there were also some species present in the cores which have recently been found southeast of the Namaqua Province along the warm temperate to subtropical coast from Algoa Province to Indo-Pacific Province, for example, *Amphibalanus amphitrite*, *Assiminea ovata, Carditopsis rugosa, Hiatula capensis*, *Loripes clausus, Moerella tulipa*, and *Pallidea palliderosea,* and *Striostrea margaritacea*.

3.4 Sea-level index points

In this study, only well preserved,^{14}C-dated shell samples and peat samples were selected for reconstruction of the relative sea-level. They indicate relative sea levels of 0.36 ± 0.56 m MSL to 2.01 ± 0.62 m MSL between 1261 cal yr BP and 161 cal yr BP in Conception Bay, −0.701 ± 0.23 m MSL (1341 cal yr BP) to −0.21 ± 0.23 m MSL (733 cal yr BP) between Sandwich Bay and Walvis Bay, and 1.12 ± 0.57 m MSL to 2.39 ± 0.57 m MSL between 5279 cal yr BP and 4916 cal yr BP in Cape Cross. The data set for Sandwich Bay was not considered (classified as rejected in the HOLSEA spreadsheet) due to the fact that the elevation measurements from the SRTM-DEM were beyond reasonable uncertainties. The data from previous studies show a larger variety of sea-level indications as well (between −2 and +6.5 m MSL) but in general, a rough trend in the data is perceptible. To verify this presumption the results of all studies have been taken for a combined calculation of the floating mean over seven values (see black line in Figure 7) which compensates for the strong variations and provides a first approximate estimation of mid to late Holocene sea-level fluctuations along the southwestern African coast.

4 Discussion

4.1 Evolution of lagoons and coastal pans

Lagoon formation starts with the development of a sand spit which is mostly initiated by rocky outcrops or river mouths. Due to intense northward-directed longshore transport (Garzanti et al., 2014), the sandy material can accumulate in the leeward position of the aforementioned starting points. Subsequently, as the sand spit grows and migrates a sheltered lagoonal embayment can develop in the back protected against strong wave impact by the sand spit barrier (sand spit/beach facies) which can be classified as recurved spit to flying spit (Davis & Fitzgerald 2009). Low hydrodynamics in the lagoon result in the deposition of fine-grained material and the formation of a tidal flat environment. Associated with the tidal flat facies are tidal channels as well as salt marshes. The active part of the lagoons is connected to the ocean by a tidal inlet which can temporarily be closed due to growth or lateral shift of the

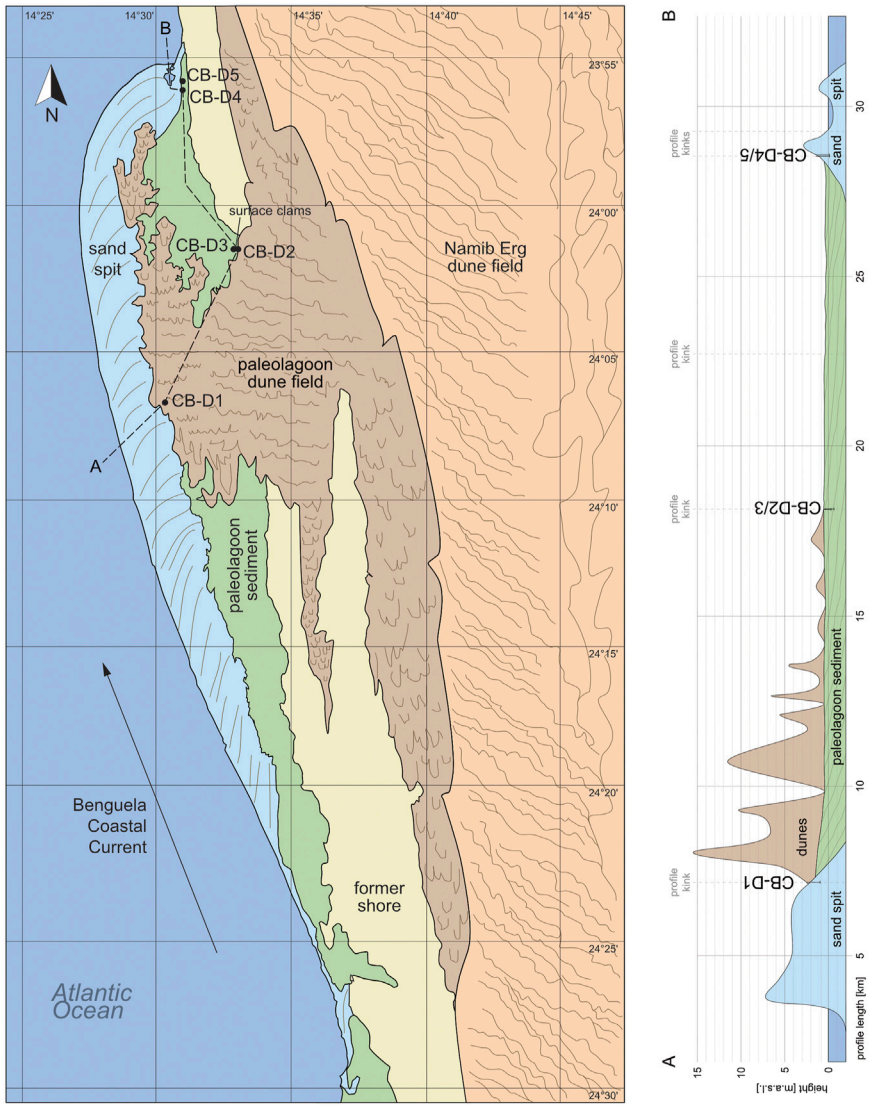

FIGURE 8
Sedimentological map and profile A-B of the basic sedimentary units in the Conception Bay paleolagoon area with locations of the sediment cores. Remote sensing mapping on the basis of various satellite images provided by Google Earth (Image Landsat/Copernicus). Validation by follow-up ground truthing.

sand spit. Consequently, the lagoons start to silt up in a northward direction. The (paleo-)lagoons investigated in this study represent different stages of lagoon development, from the fully active lagoon (Walvis Bay), to partly-active lagoons (Sandwich Bay, Conception Bay), to inactive paleolagoons like Cape Cross and Bandombay. The status of Torra Bay is still unclear as the typical structural units of a coastal lagoon in this region, such as a sand spit or a tidal flat facies, are missing. In a later phase of the paleolagoon development, the dry, flat pan-like surface is affected by eolian sediment transport; namely, dunes of different sizes, small-scale sand ripples, as well as windblown sand sheets. Additionally, overwash can occur along the sand spit barrier during high energy events (storms) and extremely high waters which lead to the formation of defined sediment fans in the back of the barrier.

The sedimentary facies defined in our study approximately correspond to the sediments from cores given by Compton (2006), Compton (2007) for the Bogenfels Pan and Anichab Pan on the southern coast of Namibia. The evaporitic pan facies (this study) combines the salt layer and pan unit of the Anichab Pan and Bogenfels Pan, respectively. Beside this, also beach deposits, shell layers of varying thickness and subtidal lagoonal deposits are mentioned. On top of the recent

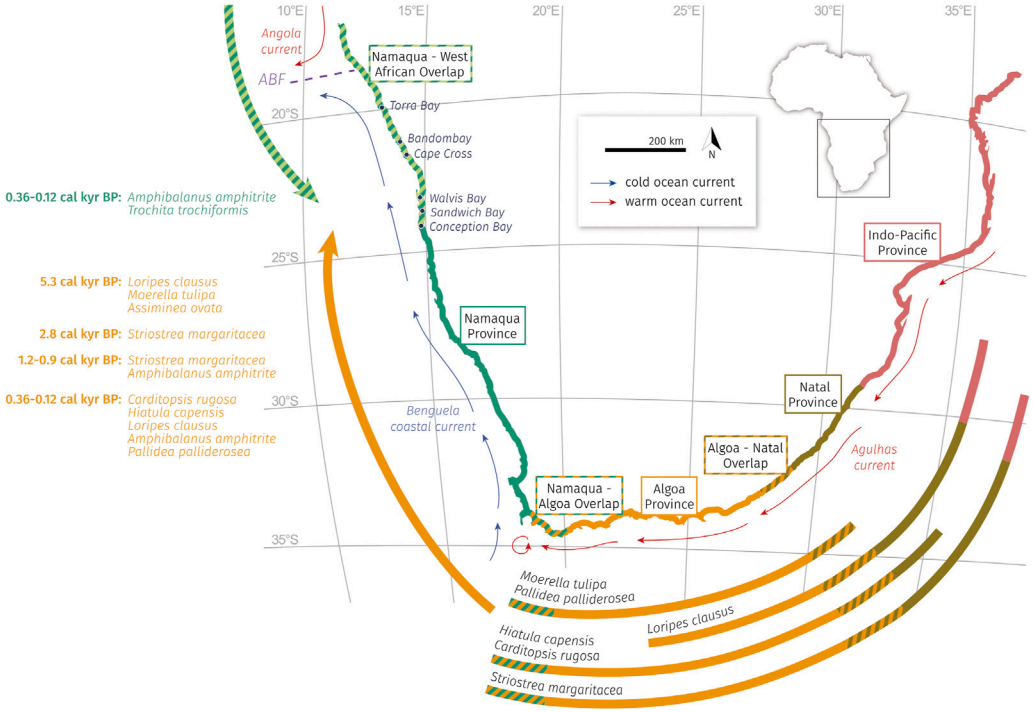

FIGURE 9
Faunal extension along the southwestern African coast since 5.7 cal ka BP. All documented species were found in the coastal pan sediments of Conception Bay, Sandwich Bay, Walvis Bay, Cape Cross, and Torra Bay. The biogeographic analyses of this study resulted in the identification of eight species from the warmer water masses of the Agulhas Current and two species that migrated from the tropical Angola basin in the north, both in the distinct time slots of 5.3 cal kyr BP, 2.8 cal kyr BP, 1.2–0.9 cal kyr BP, and 0.36–0.12 cal kyr BP. Definition of the marine provinces by Kilburn and Rippey (1982).

pan surface high mobile sand dunes were observed from both pans which corresponds to the eolian dune facies (this study). However, medium to thick bedded layers of coarse sand to gravel/cobble are missing in the more northern paleolagoons (this study). This is in accordance with the different pathways the respective particle sizes take on their way from the Orange River mouth along their northbound longshore drift (Spaggiari et al., 2006; Bluck et al., 2007).

The sedimentological map and the associated profile in Figure 8 summarize the spatial distribution of the basic sedimentary units of Conception Bay. The ^{14}C ages demonstrate the successive silting-up process over time, with the oldest sediments in the deepest layers of the southernmost core and younger ages towards the top of the core and in general to the northern direction inside the (paleo-)lagoon. The oldest determined age in the center of Conception Bay (CB-D1) reveals a minimum lagoon age of 2.8 cal kyr BP, whereas the age of the initial lagoon development at the southernmost part is still unknown. The nearby Sandwich Bay contains sediments of 5.7 cal kyr BP in the southernmost parts of the pan filling.

The other lagoons and paleolagoons developed and filled at different time intervals. The oldest sediments in Walvis Bay were dated around 3.4 kyr BP, and most of the lagoon is still open to the ocean with regular flooding and sediment deposition. However, sedimentation processes are overprinted by human activities such as the construction of harbors, coastal protection structures, and salt mining fields.

The sediment core WB-D6 was taken from the river delta of the ephemeral Kuiseb River, which rarely enters the coast in the southeastern part of the Walvis Bay lagoon. The sediments strongly reflect its short-distance transport from their terrestrial source area. The delta material is characterized by eroded material from Gamsberg (mainly quartzites and mica schists) with primarily silty to fine sand grain sizes due to the source rock characteristics. The presence of the Kuiseb River played the initial role in the development of the Walvis Bay lagoon and its sediment filling.

The paleolagoons of Cape Cross, Bandombay and Torra Bay developed at the same period as Sandwich Bay, with the oldest sediments dated to around 5.3–6.0 cal kyr BP. Bandombay also contains recent sediments at the pan surface whereas the lagoons of Cape Cross, and Torra Bay apparently filled up rapidly between 6.0 and 4.9 cal kyr BP as they do not contain any sediments younger than 4.9 cal kyr BP. The palaeolagoons in the southern part of the Namibian coast show slightly older dates.

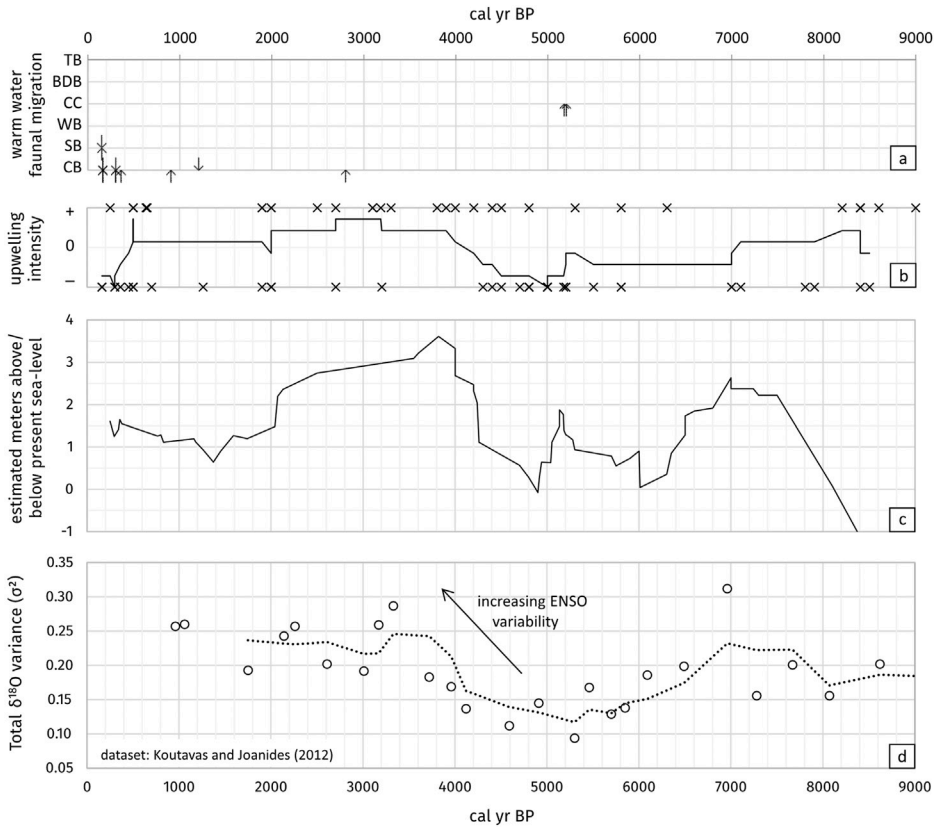

FIGURE 10
(A) Results of the biogeographic analyses of this study with age determination of the migratory fauna in the coastal lagoons (CB = Conception Bay, SB = Sandwich Bay, WB = Walvis Bay, CC = Cape Cross, BDB = Bandombay, TB = Torra Bay) and direction of movement (down arrows = extension from Angola Current, up arrows = extension from Agulhas Current). **(B)** Combined dataset from this study and other studies with information of the upwelling intensity during the last 9.0 ka BP (black crosses), "+" = stronger upwelling intensity than today, "–" = lower upwelling intensity until breakdown of the upwelling system. Solid line = floating mean over 7 values of all data (= approximate strength of the Benguela Upwelling system since 8.4 ka BP), for references see Supplementary Table S3. **(C)** Approximate Holocene sea-level curve since 9.0 ka BP (compare Figure 7, for references see Table 3). **(D)** Holocene ENSO variability from variance in $\delta^{18}O$ in individual foraminifera (*Globigerinoides ruber*) records from the equatorial eastern Pacific (dataset: Koutavas and Joanides 2012), dashed line = floating mean over 3 values.

In the southernmost Bogenfels Pan (27°28'S), *in situ* articulated shells were dated to between 7.3 and 6.5 ka cal BP and transported shell material to between 4.8 and 4.2 ka cal BP (Compton, 2006). Formation of the Anichab Pan (26°16'S) started around 7.0 ka cal BP and continued between 6.6 ka cal BP and 4.9 ka cal BP as indicated by transported shell material and bivalves in life position, respectively (Compton, 2007).

4.2 Shifts in biogeographic provinces and fluctuations in upwelling intensity

The Benguela Upwelling System (BUS) is a highly variable environment with phases of stronger and weaker upwelling intensities up to temporary total breakdown of the system. With changing upwelling intensities there are strong variations in the environmental conditions for the marine fauna (Nelson and Hutchings, 1983; Shannon, 1985; Shannon et al., 1990; Sakko, 1998; Shannon, 2001; Zhao et al., 2017). The BUS is influenced by the position and shift of the ABF at the northern margin and the Agulhas leakage at the southern. The processes and dynamics of both transition zones have been discussed in previous studies. Recently, the ABF has been situated between 14°S and 18°S but shows great temporal and spatial variability due to interannual, seasonal, as well as mesoscale controls associated with the Angola Current and the BUS (Meeuwis and Lutjeharms 1990; Lass et al., 2000). The Agulhas leakage transports heat and salt from the Indian Ocean into the highly productive BUS as well as the South Atlantic Ocean. The upper ocean temperature and salinity is strongly influenced by the mixing of these water masses. Through this means the Agulhas waters induce a positive density anomaly in the South Atlantic Ocean and stimulate a stronger and more stable Atlantic meridional overturning

TABLE 3 Calibrated ^{14}C-ages and related sea level indicators along the Namibian coast based on this study and previously published data.

age [cal yr BP]	± error/2σ-range [cal yr BP]	sea level [m MSL]	Material	Location (core number, core depth, context)	Reference
100	45	4.00	*Choromytilus* shell	Storm beach	Miller et al. (1993)
143	436-45	0.88	*Burnupena papyracea*	Conception Bay D4 (130-137 cm)	This study
160	45	0.00	*Donax* shell	Back beach	Miller et al. (1993)
161	315-0	2.01	*Donax serra*	Conception Bay D4 (in life position at pan surface)	This study
174	336-0	1.83	*Choromytilus meridionalis*	Conception Bay D5 (75 cm)	This study
226	419-28	0.92	*Choromytilus meridionalis*	Conception Bay D4 (113-118 cm)	This study
249	441-50	1.68	*Lutraria lutraria*	Conception Bay (in life position at pan surface)	This study
295	473-95	1.46	*Nassarius niveus*	Conception Bay D3 (0-4 cm)	This study
340	50	2.00	Arthropod	Back beach	Vogel and Marais, (1971)
356	509-161	1.68	*Lutraria lutraria*	Conception Bay (in life position at pan surface)	This study
376	531-195	1.31	*Choromytilus meridionalis*	Conception Bay D3 (15-19 cm)	This study
765	800-716	−0.21	Peat	Peat outcrop between Sandwich Bay and Walvis Bay	This study
802	971-637	1.09	*Nassarius Niveus*	Conception Bay D2 (19 cm)	This study
830	50	0.50	*Donax* shell	Pebbly beach	Miller et al. (1993)
1,160	50	2.00	*Donax* shell	Back beach	Miller et al. (1993)
1,180	50	1.50	*Bullia digitatis*	Beach	Vogel and Visser, (1981)
1,261	1439-1065	0.36	*Choromytilus meridionalis*	Conception Bay D3 (112 cm)	This study
1,372	1413-1307	−0.71	Peat	Peat outcrop between Sandwich Bay and Walvis Bay	This study
1,450	50	1.60	*Choromytilus* shell	Buried bar	Miller et al. (1993)
1,590	50	3.65	*Choromytilus* shell	Storm beach	Miller et al. (1993)
1,740	50	0.00	Oyster shell	Shell reef top	Flemming, (1977)
2,040	60	4.00	*Bullia* shell	Storm beach	Flemming, (1977)
2,070	50	6.50	Shell	Storm beach	Flemming, (1977)
2,130	45	1.50	*Donax* shell	Buried beach	Miller et al. (1993)
2,500	n. sp.	2.00	Not specified	Estimated increase Antarctic ice volume	Goodwin, (1998), Compton, (2001)
3,550	60	4.00	Shell	Storm beach	Flemming, (1977)
3,600	50	4.50	*Choromytilus* shell	Buried beach	Miller et al. (1993)
3,820	50	2.80	*Choromytilus* shell	Buried beach	Yates et al. (1986)
4,000	60	2.00	*Choromytilus* shell	Back beach	Miller et al. (1993)
4,000	n. sp.	2.00	*Solen capensis, Venerupis corrugata*	Relative abundance of water worn shells and pebbles	Miller et al. (1995)
4,200	n. sp.	0.00	*Solen capensis, Venerupis corrugata*	Relative abundance of water worn shells and pebbles	Miller et al. (1995)
4,200	n. sp.	1.00	Not specified	Keurbooms Estuary	Reddering, (1988)
4,240	60	2.00	*Donax* shell	Buried beach	Miller et al. (1993)
4,260	60	−2.00	Shell	Lagoon	Flemming, (1977)
4,700	n. sp.	−1.00	Orange-stained shell hash layer	Bogenfels - trench	Compton, (2006)
4,800	n. sp.	0.00	Shell fragments	Bogenfels basal beach gravel	Compton, (2006)
4,900	n. sp.	−0.50	*G. matadoa*	Anichab Pan - sandbank surface	Compton, (2007)
4,916	5199-4689	2.39	*Dosinia orbignyi*	Cape Cross D2 (4 cm)	This study
4,940	60	3.60	*Patella* shell	Shell bed on beach terrace	Vogel and Visser, (1981)
5,040	5272-4830	1.96	*Dosinia orbignyi*	Cape Cross D1 (54–60 cm)	This study

(Continued on following page)

TABLE 3 (*Continued*) Calibrated ^{14}C-ages and related sea level indicators along the Namibian coast based on this study and previously published data.

age [cal yr BP]	± error/2σ-range [cal yr BP]	sea level [m MSL]	Material	Location (core number, core depth, context)	Reference
5,053	5279-4837	1.38	*Dosinia orbignyi*	Cape Cross D1 (115 cm)	This study
5,136	5345-4872	1.66	*Dosinia orbignyi*	Cape Cross D1 (87 cm)	This study
5,136	5345-4872	1.13	*Dosinia orbignyi*	Cape Cross D1 (140 cm)	This study
5,136	5345-4872	1.05	*Dosinia orbignyi*	Cape Cross D1 (148 cm)	This study
5,177	5424-4942	1.62	*Loripes clausus*	Cape Cross D2 (97 cm)	This study
5,183	5428-4949	1.00	*Dosinia orbignyi*	Cape Cross D1 (152–155 cm)	This study
5,203	5438-4964	1.27	*Choromytilus meridionalis*	Cape Cross D1 (121 cm)	This study
5,236	5460-4982	1.04	*Dosinia orbignyi*	Cape Cross D1 (149 cm)	This study
5,279	5484-5027	1.12	*Dosinia orbignyi*	Cape Cross D2 (129–134 cm)	This study
5,300	n. sp.	−0.50	*G. matadoa*	Anichab Pan - sandbank surface	Compton, (2007)
5,700	n. sp.	0.00	Not specified	Verlorenflei	Baxter and Meadows, (1999)
5,750	60	0.00	Wood	Marine gravel	Vogel and Visser, (1981)
5,900	n. sp.	2.20	*Loripes clausus*	Keurbooms Estuary - estuarine mudbank	Reddering, (1988)
6,000	n. sp.	2.50	Shells	Archaeological evidence from shell midden	Miller et al. (1995)
6,010	45	−5.00	Oyster shell	Reef base	Vogel, (1970)
6,300	n. sp.	3.30	*Loripes clausus*	Knysna - estuarine mudbank	Marker and Miller, (1993)
6,350	80	3.00	*Ostrea atherstonei*	Reutersbrunn storm beach	Vogel and Visser, (1981)
6,500	n. sp.	3.00	Sediment	Coastal deposits along the West Coast	Compton, (2001), Compton, (2006), Herbert and Compton, (2007)
6,500	n. sp.	3.15	*Lutraria lutraria*	Bogenfels - North Basin	Compton, (2006)
6,600	n. sp.	3.00	*Ostreola stentina, Austromegabalanus cylindricus*	Anichab Pan - warm water fauna	Compton, (2007)
6,800	n. sp.	3.00	*Ostrea atherstonei*	Langebaan Lagoon - shell bed	Compton, (2001)
7,000	n. sp.	0.00	Not specified	Flandrian Transgression, ice sheets melting	Bard et al. (1996)
7,000	n. sp.	1.50	*Lutraria lutraria*	Bogenfels - North Basin	Compton, (2006)
7,000	n. sp.	3.00	*Ostreola stentina, Austromegabalanus cylindricus*	Anichab Pan - warm water fauna	Compton, (2007)
7,240	80	3.00	*Ostrea* shell	Storm beach	Vogel and Visser, (1981)
7,300	n. sp.	2.05	*Solen capensis*	Bogenfels - edge of the pan	Compton, (2006)
7,500	n. sp.	3.00	Sediment	Coastal deposits along the West Coast	Compton, (2001), Compton, (2006), Herbert and Compton, (2007)
8,100	0	−12.00	Peat	Lagoon	Schalke, (1973)
9,000	n. sp.	−25.00	Not specified	Mudbelt depositions	Bard et al. (1996)

circulation (Peeters et al., 2004; Dickson et al., 2010; Caley et al., 2014).

Because of the strong differences in recent conditions between the tropical environments in the Angola Basin in the north, in the vicinity of the Agulhas Current around the Cape region in the south, and the cool and nutrient-rich but often anoxic environment of the BUS, there are distinct marine provinces possessing characteristic biocenosis (Kilburn and Rippey, 1982, see also chapter "Marine Provinces"). During phases of upwelling weakening or breakdown, the environmental conditions along the Atlantic coast are characterized by higher oxygen availability and warmer water temperatures, resulting in an expansion of (sub-)tropical fauna into the recently cool temperate regions. Therefore, it is possible to reconstruct the paleo-upwelling conditions and strengths using biogeographic analyses of ^{14}C-dated shell material from sediment cores of coastal lagoons and paleolagoons to document phases of faunal expansion or shifts in biogeographic provinces and ecoregions.

In total, we identified 46 different macrobenthic species from core material, paleolagoon surfaces, shell midden, and beach debris lines. Most of them have a large spatial range and occur over several biogeographic provinces. Eight of the sampled species (except those from beach collections) occur in the (sub-) tropical water masses of the Agulhas Current south and east of South Africa (Namaqua-Algoa Overlap, Algoa Province, Algoa-Natal Overlap, Natal Province and Indo-Pacific Province): *Amphibalanus amphitrite*, *Assiminea ovata, Carditopsis rugosa, Hiatula capensis*, *Loripes clausus, Moerella tulipa*, *Pallidea palliderosea,* and *Striostrea margaritacea*. Two other species only occur in the study area or even exclusively north of it in the subtropical Angola Basin (*Amphibalanus amphitrite, Trochita trochiformis*).

The ^{14}C dating of these species revealed four main phases of faunal range expansion into the studied coastal region: 5.3 cal kyr BP, 2.8 cal kyr BP, 1.2–0.9 cal kyr BP, and 0.36–0.12 cal kyr BP (Figure 9) from both neighboring subtropical to warm-temperate water masses, namely the Angola Current and Agulhas Current (compare the diagram with migration directions of Figure 10B). Additionally, species of the (sub-)tropical Angola Basin (*Trochita trochiformis*) were found in the southernmost studied lagoon (Conception Bay) and species originating in the Agulhas system were found to the north up to Cape Cross (*Bullia tenuis, Loripes clausus*). The fact that all range expansion events occur parallel in both directions and species spread along the entire coastline does not allow for an improved estimation of the position of the ABF. With the dataset of this study a temporary and nearly complete breakdown of the entire upwelling system seems conceivable.

To compare our data with datasets of some published studies, age data of the Benguela Upwelling intensity were evaluated (see Supplementary Table S3 for data and references). As most information about upwelling history is given qualitatively without distinct data ("stronger"/"weaker") the information was categorized into classes of "upwelling increased" (+) and "upwelling weakened" (−) and plotted into a diagram against the age (see Figure 10C). To visualize the tendency of upwelling strength, a floating mean over seven values of all datasets was calculated and added to the diagram. Despite the differing sources and resolutions of the individual studies, a correlation between the approximate sea-level curve (Figure 10A) and the approximate upwelling strength (Figure 10C) is noticeable. Apparently, an increasing sea level is accompanied by an increase in upwelling intensity (or *vice versa*).

4.3 Atlantic Benguela Niño

Another observation in the BUS is the occurrence of warm episodes in austral summer once per decade (Lass et al., 2000), when warm water masses of the Angola Current intrude from the north along the Namibian shelf into the upwelling zone and may enter latitudes as far as 23°S/Walvis Bay (Moroshkin et al., 1970; Covey and Hastenrath 1978; Hagen et al., 1981; Shannon et al., 1986; Boyd et al., 1987; Nicholson and Entekhabi 1987; Shannon et al., 1987; Meeuwis and Lutjeharms 1990; Zebiak 1993; Carton and Huang 1994; Kirst et al., 1999; Kostianoy and Lutjeharms 1999; Lass et al., 2000; Mohrholz et al., 2001; Florenchie et al., 2003; Jahn et al., 2003; Rouault and Richard, 2003; West et al., 2004; Arntz et al., 2006; Shillington et al., 2006; Nicholson, 2010). These episodes are called "Benguela Niños" as an analogue to the El Niño events in the Pacific Ocean. As Benguela Niños cause rising SSTs on the shelf with a decline in upwelling activity (West et al., 2004), some recent instances resulted in a range expansion of the fauna (Gammelsrød et al., 1998), but it is unclear whether the detected warm water fauna documented in the sedimentary record of the lagoons can be related to relatively short Benguela events or longer-lasting breakdown of the upwelling system.

According to Arntz et al. (2006), Benguela Niños occur more seldomly than Pacific El Niños and do not necessarily coincide temporally. The summarized results of former studies of sea-level variations and upwelling intensity possibly contradict this point of view. Koutavas and Joanides (2012) studied the variance in δ^{18}O in individual foraminifera records (*Globigerinoides ruber*) from the equatorial eastern Pacific (see Figure 10D) to reconstruct the variability of the El Niño–Southern Oscillation (ENSO). The Holocene ENSO variability records apparently correlate roughly with the collected datasets of sea-level variations and upwelling intensity in the Benguela System and imply a connection between both the Pacific El Niño and the Atlantic Benguela Niño.

Some events in the fossil record were described in parallel for both upwelling systems such as the cold water coral growth in the Benguela system from 9.5 to 4.5 ka BP and the abrupt dieback of deep-water coral reefs after 4.5 ka BP (Tamborrino et al., 2019). The same phenomenon was described with the reefs along the Pacific Panamanian and Costa Rican coasts, which experienced an interruption in reef growth from 4.1 to 1.6 ka BP (Toth et al., 2012). The hiatus was associated with an increase in the strength and variability of the ENSO and changes in the position of the Intertropical Convergence Zone (ITCZ) (Toth et al., 2012; Toth et al., 2015). A change in the position of the ITCZ could also be the reason for the variations in the BUS as a change in the trade wind system has a direct impact on the Ekman transport, leading to different upwelling intensities which influence the SSTs and may cause a faunal range expansion along the coast.

4.4 Sea-level fluctuations

Today, the sediment surfaces of the investigated coastal pans are mainly above the current sea level. Some parts are

around 0–2 m aMSL and still flood during extreme high tide or storm events if conditions allow washing of the waves over the sand spits, a (re-)opening of the tidal inlet or pore- and groundwater seeping. However, some parts of the paleolagoon surfaces are more elevated (see Sandwich Bay (D1-D5), Walvis Bay (D1/D2 and D5/D6), and Bandombay (D1-D5)). This implies that the sea level was higher during the time of sediment deposition and lagoon filling and/or accumulation of eolian deposits on top of the original marine paleolagoon surface.

Table 3 summarizes published ^{14}C-dated postglacial sea-level indicators (shells, sediments, wood, peat, etc.) of prior studies in combination with the results of our study. Figure 7 summarizes all mentioned sea-level indicators from former studies (white circles) and our study in a range from −2 to +6.5 m MSL over the last 7,500 years. During the deglaciation, the water level increased rapidly around 10,000 a BP and reached modern conditions around 8,000–7,500 a BP (Bard et al., 1996; Compton, 2001; Compton, 2006; Compton, 2007; Herbert and Compton, 2007). Afterward, most sea-level indicators hint at a relatively stable sea level within a few meters of the present position.

The resulting curve indicates that after the deglaciation the sea level raised to nearly 3 m MSL until ~7,000 a BP. This result was also described in detail from similar settings exposed along the emergent beaches of the west coast today (Herbert and Compton, 2007) such as Bogenfels Pan (Compton, 2006) and Anichab Pan (Compton, 2007). Afterwards, the sea level decreased to ~1.0 m MSL until 6,000 a BP. This regression was also documented by different studies *via* hiatuses in sediment cores from the near offshore-situated mudbelt; these suggest widespread erosion over the mudbelt. The sea level has remained at this level between 6,000 and 4,500 a BP (Compton, 2001; Compton, 2006; Franceschini and Compton, 2006; Compton, 2007), until it rose again rapidly until 4,000 a BP to ~3.5 m MSL and stayed at 3.0 m MSL until 2,000 a BP. After 2,000 a BP the graph indicates a decrease to 1.0 m MSL until ~300 a BP.

Some studies have described a sea-level lowstand between 3,000 and 2,000 a BP with a gap of around 1,000 a in the onshore records (Illenberger and Rust, 1988; Miller et al., 1993; Miller et al., 1995; Compton, 2001; Franceschini and Compton, 2006). The dataset of our study also presents a gap between 2,800 and 1,700 a BP, but some shell datings along storm beach deposits of Miller et al. (1995) and Flemming (1977) do not support a sea-level lowstand during this time.

The majority of the sea-level data presented in our study indicate higher late to mid-Holocene sea levels than today. These interpretations could be distorted by bias due to the sampling method utilized. It is more difficult to detect and sample records of sea-level lowstands located below modern sea level than to sample on emergent pan surfaces or rocky outcrops that support good availability of highstand data. The resulting graph of the floating mean of all sea-level data (Figure 7) does not consider larger data gaps as well and perhaps pretends a relatively stable sea level without giving a hint to short-termed lowstands. Therefore, it must be taken into account that the analysis of the available data will always be an estimation of the highest sea levels during the periods without finer resolution of possible short phases of sea-level lowstands, for example, in the proposed record gap between 2,000–3,000 a BP (Illenberger and Rust, 1988; Miller et al., 1993; Miller et al., 1995; Compton, 2001; Franceschini and Compton, 2006).

5 Conclusion

This study emphasizes (paleo-)lagoons as important Holocene geoarchives along the arid and emergent Namibian coastal zone. From our data which include 26 sediment cores from six coastal (paleo-)lagoons, 56 ^{14}C age determinations of sediments and shell material have been conducted. Additionally, 221 faunal samples have been determined to contain 46 macrobenthic species and were analyzed with respect to their biogeographic range; as such, we can conclude the following:

The sediment filling of most of the studied (paleo-)lagoons started between 6.0 and 5.3 cal kyr BP under decelerated sea level rise and progressed from the south northwards until reaching the stage of paleolagoons (also termed coastal pans). Some still contain an active lagoonal area while others are filled up completely by sediments.

The biogeographic analyses of the collected shell material enabled the determination of different tropical warm-water species in a recent cool-temperate and oxygen-depleted upwelling system. The (sub-)tropical fauna likely extend their range along the coast during phases of decreased upwelling or even breakdown of the complete upwelling system. Age determinations of the species enabled the detection of four migration events at 5.3 cal kyr BP, 2.8 cal kyr BP, 1.2–0.9 cal kyr BP, and 0.36–0.12 cal kyr BP. The subtropical to warm-temperate fauna migrated from both directions, namely from the northern Angola Current as well as from the southern Agulhas Current into the study area.

The flat surface of many coastal paleolagoons is higher than the recent sea level, indicating phases of higher sea levels during the Holocene filling of the lagoons as well as accumulation of eolian sediments on top of the original lagoon surface. Shells in life position at the sediment surface and in the sedimentary record indicate higher late to mid-Holocene sea-level phases.

Holocene changes of sea level and upwelling intensity are likely connected to the variability of the El Niño–Southern Oscillation (ENSO) as well as the variability of the Benguela

Niño. The results of this study display the connection of ocean currents, atmospheric conditions, and the resulting response of the faunal systems on a larger regional scale.

Data availability statement

The original contributions presented in the study are included in the article/Supplementary Material, further inquiries can be directed to the corresponding author.

Author contributions

IS, LB, HW, and AW contributed to the conceptualization. IS, HW, and AW developed the methodology. IS, LB, HW, and AW carried out the investigation in the field studies. IS carried out data curation, validation, visualization, statistical analysis and wrote the first draft of the manuscript. HW and AW provided supervision. HW and AW organized funding acquisition. AW was responsible for the project administration. All authors contributed to manuscript revision, read and approved the final version of the submitted manuscript.

Funding

The study was funded in the framework of the SPACES initiative (Science Partnerships for the Assessment of Complex Earth Systems Processes) by the Federal Ministry of Education and Research (Project 03G0838B/C).

Acknowledgments

We thank the Geologic Survey of Namibia for logistic and administrative support. The Ministry of Environment and Tourism is gratefully acknowledged for giving permission for field work within the Namib-Naukluft, Dorob, and Skeleton Coast National Parks. The concession owners of the area of Conception Bay are thanked for giving access to their land and for the local support. Katja, Naude and Nils Dreyer from Walvis Bay are gratefully acknowledged for their local support, logistics, transport and guidance to Sandwich Bay and particularly to Conception Bay. Special thanks to Steffi Genderjahn, Kai Mangelsdorf, Mashal Alawi (GFZ Potsdam) and Jürgen Köster (ICBM, Oldenburg) for joint fieldwork and Torsten Janßen (SaM) and Elke Ahrensfeld (ICBM) for lab and analytic support. Thanks also to Katherine Turk (Vanderbilt University, Nashville) for linguistic proof reading. The manuscript benefited from the critical comments and constructive remarks of the reviewers Andrew Green and Aasif Mohmad Lone, which are gratefully acknowledged by the authors.

Conflict of interest

The authors declare that the research was conducted in the absence of any commercial or financial relationships that could be construed as a potential conflict of interest.

Publisher's note

Supplementary material

The Supplementary Material for this article can be found online at: https://www.frontiersin.org/articles/10.3389/feart.2022.898843/full#supplementary-material

References

Ardovini, R., and Cossignani, T. (2004). *West African seashells:(including azores, madeira and canary is.* Ankona: L'informatore piceno.

Arntz, W. E., Gallardo, V. A., Gutiérrez, D., Isla, E., Levin, L. A., Mendo, J., et al. (2006). El Niño and similar perturbation effects on the benthos of the Humboldt, California, and Benguela Current upwelling ecosystems. *Adv. Geosci.* 6, 243–265. doi:10.5194/adgeo-6-243-2006

Bard, E., Hamelin, B., Arnold, M., Montaggioni, L., Cabioch, G., Faure, G., et al. (1996). Deglacial sea-level record from Tahiti corals and the timing of global meltwater discharge. *Nature* 382 (6588), 241–244. doi:10.1038/382241a0

Baumann, K. H., and Freitag, T. (2004). Pleistocene fluctuations in the northern Benguela Current system as revealed by coccolith assemblages. *Mar. Micropaleontol.* 52 (1-4), 195–215. doi:10.1016/j.marmicro.2004.04.011

Baxter, A. J., and Meadows, M. E. (1999). Evidence for Holocene sea level change at verlorenvlei, Western cape, South Africa. *Quat. Int.* 56 (1), 65–79. doi:10.1016/s1040-6182(98)00019-6

Berger, W. H., and Wefer, G. (2002). On the reconstruction of upwelling history: Namibia upwelling in context. *Mar. Geol.* 180 (1-4), 3–28. doi:10.1016/s0025-3227(01)00203-1

Bluck, B. J., Ward, J. D., Cartwright, J., and Swart, R. (2007). The Orange River, southern Africa: An extreme example of a wave-dominated sediment dispersal system in the South Atlantic Ocean. *J. Geol. Soc.* 164 (2), 341–351. doi:10.1144/0016-76492005-189

Boyd, A. J., Salat, J., and Masó, M. (1987). The seasonal intrusion of relatively saline water on the shelf off northern and central Namibia. *South Afr. J. Mar. Sci.* 5 (1), 107–120. doi:10.2989/025776187784522577

Branch, G. M., Griffiths, C. L., Branch, M. L., and Beckley, L. E. (1994). *Two oceans, a guide to the marine life of southern Africa*. Cape Town: David Philip, 360.

Brock, F., Higham, T., Ditchfield, P., and Ramsey, C. B. (2010). Current pretreatment methods for AMS radiocarbon dating at the Oxford radiocarbon accelerator unit (ORAU). *Radiocarbon* 52 (1), 103–112. doi:10.1017/s0033822200045069

Buzer, J. S., and Sym, S. D. (1983). Diatoms and pollen in a trial core from Sandwich harbour, south west Africa (Namibia). *Br. Phycol. J.* 18 (2), 121–129. doi:10.1080/00071618300650161

Caley, T., Peeters, F. J. C., Biastoch, A., Rossignol, L., Van Sebille, E., Durgadoo, J., et al. (2014). Quantitative estimate of the paleo-Agulhas leakage. *Geophys. Res. Lett.* 41, 1238–1246. doi:10.1002/2014gl059278

Carton, J. A., and Huang, B. (1994). Warm events in the tropical Atlantic. *J. Phys. Oceanogr.* 24 (5), 888–903. doi:10.1175/1520-0485(1994)024<0888:weitta>2.0.co;2

Cohen, A. L., Parkington, J. E., Brundrit, G. B., and van der Merwe, N. J. (1992). A Holocene marine climate record in mollusc shells from the southwest African coast. *Quat. Res.* 38 (3), 379–385. doi:10.1016/0033-5894(92)90046-l

Cohen, A. L., and Tyson, P. D. (1995). Sea-surface temperature fluctuations during the holocene off the south coast of Africa: Implications for terrestrial climate and rainfall. *Holocene* 5 (3), 304–312. doi:10.1177/095968369500500305

Compton, J. S., and Franceschini, G. (2005). Holocene geoarchaeology of the sixteen mile beach barrier dunes in the Western Cape, South Africa. *Quat. Res.* 63 (1), 99–107. doi:10.1016/j.yqres.2004.09.006

Compton, J. S. (2007). Holocene evolution of the Anichab Pan on the south-west coast of Namibia. *Sedimentology* 54 (1), 55–70. doi:10.1111/j.1365-3091.2006.00826.x

Compton, J. S. (2001). Holocene sea-level fluctuations inferred from the evolution of depositional environments of the southern Langebaan Lagoon salt marsh, South Africa. *Holocene* 11 (4), 395–405. doi:10.1191/095968301678302832

Compton, J. S. (2006). The mid-Holocene sea-level highstand at Bogenfels Pan on the southwest coast of Namibia. *Quat. Res.* 66 (2), 303–310. doi:10.1016/j.yqres.2006.05.002

Cooper, J. A. G., Green, A. N., and Compton, J. S. (2018). Sea-level change in southern Africa since the last glacial maximum. *Quat. Sci. Rev.* 201, 303–318. doi:10.1016/j.quascirev.2018.10.013

Covey, D. L., and Hastenrath, S. (1978). The Pacific el nino phenomenon and the atlantic circulation. *Mon. Wea. Rev.* 106 (9), 1280–1287. doi:10.1175/1520-0493(1978)106<1280:tpenpa>2.0.co;2

Davis, R. A., Jr, and FitzGerald, D. M. (2009). *Beaches and coasts*. Oxford: Blackwell Publishing.

Dewar, G., Reimer, P. J., Sealy, J., and Woodborne, S. (2012). Late-Holocene marine radiocarbon reservoir correction (Delta R) for the west coast of South Africa. *Holocene* 22 (12), 1481–1489. doi:10.1177/0959683612449755

Dickson, A. J., Leng, M. J., Maslin, M. A., Sloane, H. J., Green, J., Bendle, J. A., et al. (2010). Atlantic overturning circulation and Agulhas leakage influences on southeast Atlantic upper ocean hydrography during marine isotope stage 11. *Paleoceanography* 25, 14. doi:10.1029/2009pa001830

Dingle, R. V., Bremner, J. M., Giraudeau, J., and Buhmann, D. (1996). Modern and palaeo-oceanographic environments under Benguela upwelling cells off southern Namibia. *Palaeogeogr. Palaeoclimatol. Palaeoecol.* 123 (1-4), 85–105. doi:10.1016/0031-0182(96)00116-2

Donn, T. E., Jr., and Cockcroft, A. C. (1989). Macrofaunal community structure and zonation of two sandy beaches on the central Namib coast, South West Africa/Namibia. *Madoqua* 1989 (2), 129–135.

Duncombe Rae, C. M. (1991). Agulhas retroflection rings in the South Atlantic Ocean: An overview. *South Afr. J. Mar. Sci.* 11 (1), 327–344. doi:10.2989/025776191784287574

Embley, R. W., and Morley, J. J. (1980). Quaternary sedimentation and paleoenvironmental studies off Namibia (South-West Africa). *Mar. Geol.* 36 (3-4), 183–204. doi:10.1016/0025-3227(80)90086-9

Emeis, K. C., Struck, U., Leipe, T., and Ferdelman, T. G. (2009). Variability in upwelling intensity and nutrient regime in the coastal upwelling system offshore Namibia: Results from sediment archives. *Int. J. Earth Sci.* 98 (2), 309–326. doi:10.1007/s00531-007-0236-5

Farmer, E. C., Demenocal, P. B., and Marchitto, T. M. (2005). Holocene and deglacial ocean temperature variability in the Benguela upwelling region: Implications for low-latitude atmospheric circulation. *Paleoceanography* 20 (2). doi:10.1029/2004pa001049

Farr, T. G., Rosen, P. A., Caro, E., Crippen, R., Duren, R., Hensley, S., et al. (2007). The shuttle radar topography mission. *Rev. Geophys.* 45 (2), RG2004. doi:10.1029/2005rg000183

Flemming, B. W. (1977). Langebaan lagoon: A mixed carbonate-siliciclastic tidal environment in a semi-arid climate. *Sediment. Geol.* 18 (1-3), 61–95. doi:10.1016/0037-0738(77)90006-9

Florenchie, P., Lutjeharms, J. R., Reason, C. J. C., Masson, S., and Rouault, M. (2003). The source of Benguela Niños in the South Atlantic Ocean. *Geophys. Res. Lett.* 30 (10). doi:10.1029/2003gl017172

Franceschini, G., and Compton, J. S. (2006). Holocene evolution of the sixteen mile beach complex, Western Cape, South Africa. *J. Coast. Res.* 22 (5), 1158–1166. doi:10.2112/05-0576.1

Gammelsrød, T., Bartholomae, C. H., Boyer, D. C., Filipe, V. L. L., and O'toole, M. J. (1998). Intrusion of warm surface water along the Angolan Namibian coast in february–march 1995: The 1995 Benguela Niño. *South Afr. J. Mar. Sci.* 19, 41–56. doi:10.2989/025776198784126719

Garzanti, E., Vermeesch, P., Andò, S., Lustrino, M., Padoan, M., and Vezzoli, G. (2014). Ultra-long distance littoral transport of Orange sand and provenance of the Skeleton Coast Erg (Namibia). *Mar. Geol.* 357, 25–36. doi:10.1016/j.margeo.2014.07.005

Gibson, R., Hextall, B., and Rogers, A. (2001). *Photographic guide to the sea and shore life of britain and northwest europe*. Oxford: University Press.

Goodwin, I. D. (1998). Did changes in Antarctic ice volume influence late Holocene sea-level lowering? *Quat. Sci. Rev.* 17 (4-5), 319–332. doi:10.1016/s0277-3791(97)00051-6

Hagen, E., Schemainda, R., Michelsen, N., Postel, L., Schulz, S., and Below, M. (1981). Zur küstensenkrechten Struktur des Kaltwasserauftriebs vor der Küste Namibias. Nationalkomitee für Geodäsie u. Geophysik bei d. Akad. *D. Wiss. D. DDR.*

Hay, W. W., and Brock, J. C. (1992). Temporal variation in intensity of upwelling off southwest Africa. *Geol. Soc. Lond. Spec. Publ.* 64 (1), 463–497. doi:10.1144/gsl.sp.1992.064.01.31

Heaton, T. J., Köhler, P., Butzin, M., Bard, E., Reimer, R. W., Austin, W. E. N., et al. (2020). Marine20 - the marine radiocarbon age calibration curve (0-55, 000 cal BP). *Radiocarbon* 62, 779–820. doi:10.1017/RDC.2020.68

Heinrich, S., Zonneveld, K. A., Bickert, T., and Willems, H. (2011). The Benguela upwelling related to the miocene cooling events and the development of the antarctic circumpolar current: Evidence from calcareous dinoflagellate cysts. *Paleoceanography* 26 (3). doi:10.1029/2010pa002065

Herbert, C. T., and Compton, J. S. (2007). Geochronology of holocene sediments on the Western margin of South Africa. *South Afr. J. Geol.* 110 (2-3), 327–338. doi:10.2113/gssajg.110.2-3.327

Heyns-Veale, E. R., Bernard, A. T. F., Midgley, J. M., and Herbert, D. G. (2022). The distribution of offshore benthic molluscs provides new insight into South Africa's marine biogeography. *Ocean Coast. Manag.* 217, 106001. doi:10.1016/j.ocecoaman.2021.106001

Hijma, M. P., Engelhart, S. E., Törnqvist, T. E., Horton, B. P., Hu, P., and Hill, D. F. (2015). "A protocol for a geological sea-level database," in *Handbook of sea-level research*. Editors I. Shennan, A. J. Long, and B. P. Horton (Hoboken: John Wiley & Sons), 536–554.

Hogg, A. G., Heaton, T. J., Hua, Q., Palmer, J. G., Turney, C. S. M., Southon, J., et al. (2020). SHCal20 Southern Hemisphere calibration, 0-55, 000 years cal BP. *Radiocarbon* 62, 759–778. doi:10.1017/RDC.2020.59

Illenberger, W. K., and Rust, I. C. (1988). A sand budget for the Alexandria coastal dunefield, South Africa. *Sedimentology* 35 (3), 513–521. doi:10.1111/j.1365-3091.1988.tb01001.x

Jahn, B., Donner, B., Müller, P. J., Röhl, U., Schneider, R. R., and Wefer, G. (2003). Pleistocene variations in dust input and marine productivity in the northern Benguela current: Evidence of evolution of global glacial–interglacial cycles. *Palaeogeogr. Palaeoclimatol. Palaeoecol.* 193 (3-4), 515–533. doi:10.1016/s0031-0182(03)00264-5

Jury, M. R. (2017). Coastal upwelling at Cape Frio: Its structure and weakening. *Cont. Shelf Res.* 132, 19–28. doi:10.1016/j.csr.2016.11.009

Kostianoy, A. G., and Lutjeharms, J. R. E. (1999). Atmospheric effects in the Angola-Benguela frontal zone. *J. Geophys. Res.* 104 (C9), 20963–20970. doi:10.1029/1999jc900017

Kensley, B. F., and Penrith, M. (1977). Biological survey of Sandvis 1, introduction and faunal list. *Madoqua* 1977 (3), 181–190.

Khan, N. S., Horton, B. P., Engelhart, S., Rovere, A., Vacchi, M., Ashe, E. L., et al.the HOLSEA working group (2019). Inception of a global atlas of sea levels since the Last Glacial Maximum. *Quat. Sci. Rev.* 220, 359–371. doi:10.1016/j.quascirev.2019.07.016

Kiessling, A. (2002). *Sedimentphysikalische Eigenschaften auf dem Schelf und oberen Kontinentalrand von Namibia - auswertung von Sedimentkernen der Reise METEOR 48-2. M. Sc. Thesis*. Greifswald: Greifswald University, 66.

Kilburn, R., and Rippey, E. (1982). *Sea shells of southern Africa*. Johannesburg: Macmillan.

Kim, J. H., Schneider, R. R., Müller, P. J., and Wefer, G. (2002). Interhemispheric comparison of deglacial sea-surface temperature patterns in Atlantic eastern boundary currents. *Earth Planet. Sci. Lett.* 194 (3-4), 383–393. doi:10.1016/s0012-821x(01)00545-3

Kirst, G. J., Schneider, R. R., Müller, P. J., von Storch, I., and Wefer, G. (1999). Late quaternary temperature variability in the Benguela current system derived from alkenones. *Quat. Res.* 52 (1), 92–103. doi:10.1006/qres.1999.2040

Koutavas, A., and Joanides, S. (2012). El Niño–Southern oscillation extrema in the holocene and last glacial maximum. *Paleoceanography* 27 (4). doi:10.1029/2012pa002378

Lamy, F., Hebbeln, D., Röhl, U., and Wefer, G. (2001). Holocene rainfall variability in southern Chile: A marine record of latitudinal shifts of the southern westerlies. *Earth Planet. Sci. Lett.* 185 (3-4), 369–382. doi:10.1016/s0012-821x(00)00381-2

Lass, H. U., Schmidt, M., Mohrholz, V., and Nausch, G. (2000). Hydrographic and current measurements in the area of the Angola–Benguela front. *J. Phys. Oceanogr.* 30 (10), 2589–2609. doi:10.1175/1520-0485(2000)030<2589:hacmit>2.0.co;2

Leduc, G., Herbert, C. T., Blanz, T., Martinez, P., and Schneider, R. (2010). Contrasting evolution of sea surface temperature in the Benguela upwelling system under natural and anthropogenic climate forcings. *Geophys. Res. Lett.* 37 (20). doi:10.1029/2010gl044353

Lutjeharms, J. R. E., and Meeuwis, J. M. (1987). The extent and variability of South-East Atlantic upwelling. *South Afr. J. Mar. Sci.* 5 (1), 51–62. doi:10.2989/025776187784522621

Lutjeharms, J. R. E., and Van Ballegooyen, R. C. (1988). Anomalous upstream retroflection in the Agulhas current. *Science* 240 (4860), 1770. doi:10.1126/science.240.4860.1770

Martínez-Méndez, G., Zahn, R., Hall, I. R., Peeters, F. J. C., Pena, L. D., Cacho, I., et al. (2010). Contrasting multiproxy reconstructions of surface ocean hydrography in the Agulhas Corridor and implications for the Agulhas Leakage during the last 345, 000 years. *Paleoceanography* 25, PA4227. doi:10.1029/2009pa001879

Martínez-Méndez, G., Zahn, R., Hall, I. R., Pena, L. D., and Cacho, I. (2008). 345, 000-year-long multi-proxy records off south Africa document variable contributions of northern versus southern component water to the deep South Atlantic. *Earth Planet. Sci. Lett.* 267, 309–321. doi:10.1016/j.epsl.2007.11.050

Meeuwis, J. M., and Lutjeharms, J. R. E. (1990). Surface thermal characteristics of the Angola-Benguela front. *South Afr. J. Mar. Sci.* 9 (1), 261–279. doi:10.2989/025776190784378772

Meisel, S., Emeis, K. C., Struck, U., and Kristen, I. (2011). Nutrient regime and upwelling in the northern Benguela since the middle Holocene in a global context–a multi-proxy approach. *Foss. Rec.* 14 (2), 171–193. doi:10.1002/mmng.201100006

Miller, D. E., Yates, R. J., Parkington, J. E., and Vogel, J. (1993). Radiocarbon-dated evidence relating to a mid-Holocene relative high sea-level on the south-Western Cape coast, South Africa. *South Afr. J. Sci.* 89 (1), 35–44.

Miller, D. E., Yates, R. J., Jerardino, A., and Parkington, J. E. (1995). Late holocene coastal change in the southwestern cape, south Africa. *Quat. Int.* 29, 3–10. doi:10.1016/1040-6182(95)00002-z

Mohrholz, V., Schmidt, M., and Lutjeharms, J. R. E. (2001). The hydrography and dynamics of the Angola-Benguela frontal zone and environment in april 1999: BENEFIT marine science. *South Afr. J. Sci.* 97 (5), 199–208.

Moroshkin, K. V., Bubnov, V. A., and Bulatov, R. P. (1970). Water circulation in the eastern South Atlantic ocean. *OCEANOLOGY* 10 (1), 27–34. 8 P, 4 FIG, 13 REF.

Nelson, G., and Hutchings, L. (1983). The Benguela upwelling area. *Prog. Oceanogr.* 12 (3), 333–356. doi:10.1016/0079-6611(83)90013-7

Nicholson, S. E. (2010). A low-level jet along the Benguela coast, an integral part of the Benguela current ecosystem. *Clim. Change* 99 (3), 613–624. doi:10.1007/s10584-009-9678-z

Nicholson, S. E., and Entekhabi, D. (1987). Rainfall variability in equatorial and southern Africa: Relationships with sea surface temperatures along the southwestern coast of Africa. *J. Clim. Appl. Meteor.* 26 (5), 561–578. doi:10.1175/1520-0450(1987)026<0561:rvieas>2.0.co;2

Peeters, F. J. C., Acheson, R., Brummer, G.-J. A., de Ruijter, W. P. M., Schneider, R. R., Ganssen, G. M., et al. (2004). Vigorous exchange between the Indian and Atlantic oceans at the end of the past five glacial periods. *Nature* 430, 661–665. doi:10.1038/nature02785

Pether, J. (1994). *The sedimentology, palaeontology and stratigraphy of coastal-plain deposits at Hondeklip Bay, Namaqualand, South Africa (Master's thesis*. Cape Town: University of Cape Town.

Petrick, B. F., McClymont, E. L., Marret, F., and andvan der Meer, M. T. J. (2015). Changing surface water conditions for the last 500 ka in the Southeast Atlantic: Implications for variable influences of Agulhas leakage and Benguela upwelling. *Paleoceanography* 30, 1153–1167. doi:10.1002/2015PA002787

Reddering, J. S. V. (1988). Coastal and catchment basin controls on estuary morphology of the south-eastern Cape coast. *South Afr. J. Sci.* 84 (3).

Rouault, M., and Richard, Y. (2003). Intensity and spatial extension of drought in South Africa at different time scales. *Water sa.* 29 (4), 489–500. doi:10.4314/wsa.v29i4.5057

Sakko, A. L. (1998). The influence of the Benguela upwelling system on Namibia's marine biodiversity. *Biodivers. Conservation* 7 (4), 419–433. doi:10.1023/a:1008867310010

Shannon, L. V., Agenbag, J. J., and Buys, M. E. L. (1987). Large-and mesoscale features of the Angola-Benguela front. *South Afr. J. Mar. Sci.* 5 (1), 11–34. doi:10.2989/025776187784522261

Shannon, L. V., Agenbag, J. J., Walker, N. D., and Lutjeharms, J. R. E. (1990). A major perturbation in the Agulhas retroflection area in 1986. *Deep Sea Res. Part A. Oceanogr. Res. Pap.* 37 (3), 493–512. doi:10.1016/0198-0149(90)90021-m

Shannon, L. V. (2001). "Benguela current," in *Encyclopedia of ocean sciences*. Editors K. C. Cochran, H. J. Bokuniewicz, and P. L. Yager. 3rd edition (Academic Press), 291–302.

Shannon, L. V., Boyd, A. J., Brundrit, G. B., and Taunton-Clark, J. (1986). On the existence of an El Niño-type phenomenon in the Benguela system. *J. Mar. Res.* 44 (3), 495–520. doi:10.1357/002224086788403105

Shannon, L. V., and Nelson, G. (1996). "The Benguela: Large scale features and processes and system variability," in *The south atlantic* (Berlin, Heidelberg: Springer), 163–210.

Shannon, L. V., Payne, A. I. L., and Crawford, R. J. H. (1989). *The physical environment. Oceans of life off southern Africa*, 12–27.

Shannon, L. V. (1985). The Benguela ecosystem. Part I: Evolution of the Benguela physical features and processes. *Oceanogr. Mar. Biol.* 23, 105–182.

Shi, N., Dupont, L. M., Beug, H. J., and Schneider, R. (2000). Correlation between vegetation in southwestern Africa and oceanic upwelling in the past 21, 000 years. *Quat. Res.* 54 (1), 72–80. doi:10.1006/qres.2000.2145

Shillington, F. A., Reason, C. J. C., Rae, C. D., Florenchie, P., and Penven, P. (2006). *4 large scale physical variability of the Benguela current large marine ecosystem (BCLME)*, 14. Elsevier, 49–70. Large marine ecosystems.

Spaggiari, R. I., Bluck, B. J., and Ward, J. D. (2006). Characteristics of diamondiferous Plio-Pleistocene littoral deposits within the palaeo-Orange River mouth, Namibia. *Ore Geol. Rev.* 28 (4), 475–492. doi:10.1016/j.oregeorev.2005.03.011

Summerhayes, C. P. (1983). Sedimentation of organic matter in upwelling regimes. *Coast. upwelling–Its Sediments Rec. Part B Sediment. Rec. Anc. Coast. upwelling* 1, 29–72.

Summerhayes, C. P., Kroon, D., Rosell-Melé, A., Jordan, R. W., Schrader, H. J., Hearn, R., et al. (1995). Variability in the Benguela Current upwelling system over the past 70, 000 years. *Prog. Oceanogr.* 35 (3), 207–251. doi:10.1016/0079-6611(95)00008-5

Tamborrino, L., Wienberg, C., Titschack, J., Wintersteller, P., Mienis, F., Schröder-Ritzrau, A., et al. (2019). Mid-Holocene extinction of cold-water corals on the Namibian shelf steered by the Benguela oxygen minimum zone. *Geology* 47 (12), 1185–1188. doi:10.1130/g46672.1

Tankard, A. J. (1975). The marine neogene saldanha formation. *South Afr. J. Geol.* 78 (2), 257–264.

Tebble, N. (1976). *British bivalve seashells; a handbook for identification*. Edinburgh: Her Majesty's Stationery Office.

Toth, L. T., Aronson, R. B., Cobb, K. M., Cheng, H., Edwards, R. L., Grothe, P. R., et al. (2015). Climatic and biotic thresholds of coral-reef shutdown. *Nat. Clim. Change* 5 (4), 369–374. doi:10.1038/nclimate2541

Toth, L. T., Aronson, R. B., Vollmer, S. V., Hobbs, J. W., Urrego, D. H., Cheng, H., et al. (2012). ENSO drove 2500-year collapse of eastern Pacific coral reefs. *Science* 337 (6090), 81–84. doi:10.1126/science.1221168

Vogel, J. C., and Marais, M. (1971). Pretoria radiocarbon dates I. *Radiocarbon* 13 (2), 378–394. doi:10.1017/s003382220000850x

Vogel, J. C., and Visser, E. (1981). Pretoria radiocarbon dates II. *Radiocarbon* 23 (1), 43–80. doi:10.1017/s0033822200037462

Vogel, J. (1970). Groningen radiocarbon dates IX. *Radiocarbon* 12 (2), 444–471. doi:10.1017/s0033822200008183

Wearne, K., and Underhill, L. G. (2005). Walvis bay, Namibia: A key wetland for waders and other coastal birds in southern Africa. *Bulletin-wader Study Group* 107, 24.

Weldeab, S., Stuut, J. B., Schneider, R. R., and Siebel, W. (2013). Holocene climate variability in the winter rainfall zone of South Africa. *Clim. Past.* 9 (5), 2347–2364. doi:10.5194/cp-9-2347-2013

West, S., Jansen, J. H. F., and Stuut, J. B. (2004). Surface water conditions in the Northern Benguela Region (SE Atlantic) during the last 450 ky reconstructed from assemblages of planktonic foraminifera. *Mar. Micropaleontol.* 51 (3-4), 321–344. doi:10.1016/j.marmicro.2004.01.004

WoRMS Editorial Board (2022). World register of marine species. at VLIZ. Available from http://www.marinespecies.org (Accessed 02 28, 2022).

Yates, R. J., Miller, D. E., Halkett, D. J., Manhire, A. H., Parkington, J. E., and Vogel, J. C. (1986). A late midholocene high sea-level-A preliminary-report on geoarchaelogy at elands bay, western cape-province, south-africa. *South Afr. J. Sci.* 82 (3), 164–165.

Zebiak, S. E. (1993). Air–sea interaction in the equatorial Atlantic region. *J. Clim.* 6 (8), 1567–1586. doi:10.1175/1520-0442(1993)006<1567:aiitea>2.0.co;2

Zhao, X., Dupont, L., Meadows, M. E., and Wefer, G. (2016). Pollen distribution in the marine surface sediments of the mudbelt along the west coast of South Africa. *Quat. Int.* 404, 44–56. doi:10.1016/j.quaint.2015.09.032

Zhao, X., Dupont, L., Schefuß, E., Bouimetarhan, I., and Wefer, G. (2017). Palynological evidence for Holocene climatic and oceanographic changes off Western South Africa. *Quat. Sci. Rev.* 165, 88–101. doi:10.1016/j.quascirev.2017.04.022